DEFORMATION PROCESSES OF ZIRCONIUM

by

Eugene John Rapperport

S. B. Massachusetts Institute of Technology

1952

Submitted in Partial Fulfillment of the

Requirements for the Degree of

Doctor of Science

from

Massachusetts Institute of Technology

1955

Author . . . Signature redacted
Department of Metallurgy

Thesis Supervisor . . . Signature redacted

Chairman, Department Committee on Graduate Students . . . Signature redacted

Metall

Thesis

1955

MASS.
AUG 1
LIBRARY

DEFORMATION PROCESSES OF ZIRCONIUM

Eugene J. Rapperport

Submitted to the Department of Metallurgy on May 9, 1955, in partial fulfillment of the requirements for the Degree of Doctor of Science.

Abstract

The deformation processes active in zirconium deformed at room temperature have been examined. Tension and compression tests were performed on single crystals and large grained samples of crystal bar zirconium and arc-melted crystal bar zirconium. After removal of hydrogen from the samples, two methods of crystal production were used. One was to heat the samples in vacuo for eight to ten days at 840° C; the other was to cycle the samples one to three times between four hours at 1200° C, and five to ten days at 840° C.

The only slip system observed at room temperature was $(10\bar{1}0)$ $[\bar{1}2\bar{1}0]$, with a critical resolved shear stress for slip of about 0.65 Kg/mm^2 in compression. The twin planes observed were $\{10\bar{1}2\}$, $\{11\bar{2}1\}$, $\{11\bar{2}2\}$, and $\{11\bar{2}3\}$. The twin parameters - K_1, η_1, K_2, η_2 and shear magnitude - were determined experimentally for $\{10\bar{1}2\}$ and $\{11\bar{2}2\}$ twins, and a tentative value for the shear magnitude was obtained for $\{11\bar{2}1\}$ twinning.

Lindgren (metal) Aug 13, 1955

In addition to the use of conventional stereographic analysis, two vector analysis methods were developed for the solution of twin indices. Approximate thicknesses were found for $\{10\bar{1}2\}$, $\{11\bar{2}1\}$, and $\{11\bar{2}2\}$ twins, and it was observed that there was an inverse relationship between twinning shear and twin thickness.

Thesis Supervisor: Albert R. Kaufmann
Associate Professor of Metallurgy
Massachusetts Institute of Technology

Table of Contents

Table of Contents, Cont'd.

Table of Contents, Cont'd.

List of Illustrations

List of Illustrations, Cont'd

List of Tables

Acknowledgements

The author wishes to acknowledge his indebtedness to Professor A. R. Kaufmann, under whose direction this problem was formulated and the work performed. Thanks are given to the members of the staff of Nuclear Metals Inc. for their help and cooperation, with particular appreciation to Dr. W. L. Lees, Dr. W. B. Nowak, and Mr. J. L. Klein for their interest in this work and their helpful suggestions. Thanks are also given Professor E. Orowan for his stimulating discussion of the various phases of this problem. The work was done under contract AT(30-1)-981 with the United States Atomic Energy Commission.

I. Introduction

Zirconium is currently of interest because it combines some physical properties that are highly desirable in nuclear reactor applications. In particular, zirconium combines excellent corrosion resistance with a low neutron capture cross-section. This combination of properties suggests its use as a structural component in reactors. In addition to the properties mentioned, zirconium is easily formed, it has a fairly low density, and it can be strengthened considerably by alloying.

The structure of zirconium is close-packed hexagonal at temperatures below 863° C., with a c/a value of 1.5931 at 25° C. (Russell, 1954, p. 1047). Above 863° C. the metal is body-centered cubic and it melts at about 1834° C. Although zirconium is quite corrosion resistant at temperatures near room temperature, it is very reactive at elevated temperatures, tending to react with its container and to act as a scavenger for various gases such as oxygen, nitrogen, and hydrogen.

Zirconium is a transition element, having only two electrons in the 4d shell and two electrons filling the 5s shell. In this respect it is similar to titanium which has only two electrons in the 3d shell and two electrons filling the 4s shell. This similarity in electronic configuration presumably accounts for the marked similarity of the chemical and physical properties of the two metals.

Although work has been performed to determine the physical and mechanical properties of polycrystalline zirconium (Miller, 1954), very little has been done to determine the mechanisms of deformation of single crystals of the metal. One reason has been the difficulty encountered in growing crystals of sufficient size. The subject of the present work is the growth of crystals of adequate size and the testing of these crystals to determine the operative deformation processes at room temperature.

The mechanics and techniques of determining the deformation processes of zirconium were very much like those used in many of the other metals whose deformation modes have been investigated. A study of this sort consists of obtaining single crystals, determining their orientations, deforming them under known conditions, and then analyzing the marks and traces left on the sample surfaces. Some innovations and modifications of procedure were made in this work, and some interesting and unusual deformation systems were found. The great majority of data reported for deformation processes in close-packed hexagonal metals show slip occurring on the (0001) plane and twinning on the $\{10\bar{1}2\}$ planes. However, in this work zirconium showed no (0001) slip, and $\{10\bar{1}2\}$ was only one of four observed twin planes.

All work was done at room temperature on the purest available zirconium. The slip and twin systems reported were produced by controlled mechanical deformation; no

extensive experiments were performed to determine the effect of incidental deformations, such as those caused by abrasion or thermal stresses.

II. Discussion of Previous Recorded Work

Very little work has been reported in the determination of the deformation processes of zirconium. The only recorded work found at the time of this writing was by F. D. Rosi (personal communication to A. R. Kaufmann, 1953). This work stated that at room temperature slip occurred predominantly on planes of the form $\{10\bar{1}0\}$ and twins occurred on planes of the forms $\{10\bar{1}2\}$ and $\{11\bar{2}1\}$. In addition, Rosi suspected the presence of $\{10\bar{1}1\}$ slip and $\{11\bar{2}2\}$ twinning, although he had not found these planes experimentally.

Titanium is a close-packed hexagonal metal that behaves chemically and physically very much like zirconium. The c/a value for titanium at 25° C. is 1.5873, which is quite close to the 1.5931 value for zirconium at the same temperature. Both elements are in Group IV-A of the periodic table; both elements have two electrons in an outermost d shell and two electrons filling the following s shell. For these reasons the literature concerning the deformation processes of titanium was surveyed with care. Titanium, also, proved to be a metal with somewhat unusual deformation modes, similar, in fact, to those found in zirconium.

Deformation processes in coarse crystals of titanium deformed at room temperature were reported by Rosi, Dube, and Alexander (1953). The deformation processes of single

crystals and large crystals of titanium deformed at room temperature were reported by Anderson, Jillson, and Dunbar (1953), by Liu and Steinberg (1952), and by Churchman (1954). These studies are summarized in Table I.

Churchman (1954) has presented an argument to explain the variance in the active slip planes as listed in Table I. This explanation states that the interstitial impurity content affects the critical resolved shear stress for slip in the systems observed. Churchman further states that $\{10\bar{1}0\}$ is the principal slip plane and is favored by increased purity.

The direction of slip for titanium in the $\{10\bar{1}0\}$ plane has been found to be $\langle 11\bar{2}0\rangle$ (Anderson, Jillson, and Dunbar, 1953, and Churchman, 1954). The direction of slip in the $\{10\bar{1}1\}$ plane was deduced to be $\langle 11\bar{2}0\rangle$ (Rosi, Dube, and Alexander, 1953, and Churchman, 1954). The direction of slip in the basal plane was found to be $\langle 11\bar{2}0\rangle$ (Anderson, Jillson, and Dunbar, 1953, and Churchman, 1954). The critical resolved shear stress for slip in titanium was reported for the active slip planes by the above workers and is summarized in Table II.

Table I: Summary of deformation planes observed in titanium deformed at room temperature.

Mechanism	Plane	Rosi, Dube, Alexander	Liu, Steinberg	Anderson, Jillson, Dunbar	Churchman
Slip	$\{10\bar{1}0\}$	x	(a)	x	x
Slip	$\{10\bar{1}1\}$	x	(a)	(b)	x
Slip	{0001}	(b)	(a)	x	x
Twinning	$\{10\bar{1}2\}$	x	x	x	x
Twinning	$\{11\bar{2}1\}$	x	x	x	(b)
Twinning	$\{11\bar{2}2\}$	x	x	x	x
Twinning	$\{11\bar{2}3\}$	(b)	x	(b)	(b)
Twinning	$\{11\bar{2}4\}$	(b)	x	(b)	(b)

x: plane observed
(a): no slip analysis reported
(b): not reported as an active plane

Table II: Summary of the critical resolved shear stresses required for slip on the active planes of titanium deformed at room temperature.

Slip Plane	Investigator	Direction of Stress	Average Value (Kg/mm^2)	Minimum Value (Kg/mm^2)
$\{10\bar{1}0\}$	Anderson, Jillson, Dunbar	Tension	5.3	4.5
	Anderson, Jillson, Dunbar	Compression	6.5 (a)	6.5 (a)
	Churchman	Tension	9.2	1.4
$\{10\bar{1}1\}$	Churchman	Tension	9.9	---
{0001}	Anderson, Jillson, Dunbar	Tension	12.5	10.1
	Churchman	Tension	10.9	6.3

(a) only one value reported

The twinning indices other than the composition plane have not been reported on the basis of experimental data for either titanium or zirconium. However, there has been speculation of some of the other indices based on crystallographic geometry (Hall, 1954, and Rosi, Dube, and Alexander, 1953). Cahn (1954) has given some criticism of the use of crystal geometry to determine twinning indices in the absence of experimental data.

Some work has also been reported on the mechanisms of deformation operative in titanium deformed at elevated temperatures (McHargue and Hammond, 1953) in which it was found that no new deformation modes occurred.

It is to be noted that the slip systems and twin systems described above for titanium are quite different from those found in other close-packed hexagonal metals. Tabulations of slip and twin systems are given for some close-packed hexagonal metals by Barrett (1952), Hall (1954), and Schmid and Boas (1935). All the close-packed hexagonal metals listed by these authors have predominantly the (0001) $[11\bar{2}0]$ slip system and a $\{10\bar{1}2\}$ twin plane active. Some exceptions to this generality have been found; however, none of the exceptions have the variety of active planes that have been found in zirconium and titanium.

Table III is a summary of the deformation processes of some of the close-packed hexagonal metals other than titanium and zirconium. The data for this table was

obtained primarily from Barrett (1952), Hall (1954), and Schmid and Boas (1935). The data on beryllium is from Tuer (1954), and existence of $\{10\bar{1}0\}$ slip in zinc is obtained from B. Chalmers (personal communication).

Table III: Crystallography of slip and twinning for some close-packed hexagonal metals.

Metal	$\frac{c}{a}$ at room temperature	Slip Plane	Slip Direction	First Undistorted Twinning Plane K_1	Second Undistorted Twinning Plane K_2	Magnitude of Shear S
Beryllium	1.568	(0001) $(10\bar{1}0)$	$[11\bar{2}0]$ $[\bar{1}2\bar{1}0]$	$(10\bar{1}2)$	$(10\bar{1}\bar{2})$(a)	0.199
Magnesium	1.624	(0001) $(10\bar{1}1)$(b)	$[11\bar{2}0]$ $[\bar{1}2\bar{1}0]$(b)	$(10\bar{1}2)$ $(10\bar{1}1)$	$(10\bar{1}\bar{2})$(a) --	0.129
Zinc	1.856	(0001) $(10\bar{1}0)$	$[11\bar{2}0]$ $[\bar{1}2\bar{1}0]$	$(10\bar{1}2)$	$(10\bar{1}\bar{2})$	0.139
Cadmium	1.886	(0001)	$[11\bar{2}0]$	$(10\bar{1}2)$	$(10\bar{1}\bar{2})$(a)	0.171
Zn - Cd	--	--	--	$(10\bar{1}2)$	$(10\bar{1}\bar{2})$(a)	--
Zn - Sn	--	--	--	$(10\bar{1}2)$	$(10\bar{1}\bar{2})$(a)	--

(a) In these twins K_2 was not experimentally determined. In line with the experimental results on zinc, K_2 was assumed to be $(10\bar{1}\bar{2})$ and the shear calculated accordingly.

(b) Found at elevated temperatures.

III. Plan of Work

The outline given below is the general plan followed in the performance of this work.

I. Preparation of samples

A. Fabrication of sample bars

B. Removal of hydrogen from samples

C. Growth of large crystals

1) Long time anneal *in vacuo*

2) Cyclic heat treatment, annealing above and below alpha-beta transformation temperature

D. Selection of usable specimens

1) Polishing samples after growth of crystals

2) Etching to reveal grain structure

3) Selecting suitable grains for observation

E. Cutting compression samples to length and polishing ends

F. Determination of geometry of specimens

1) Measurement of dihedral angles between specimen faces

2) Preparation and analysis of Laue photographs of specimens

3) Measurement of mass and cross-sectional area

II. Deformation of specimens

A. Final electropolish

B. Alignment of deformation equipment

C. Measurements and observations on samples being deformed

1) Deformation by known tensile strains

2) Deformation by known tensile stresses

3) Deformation by known compressive stresses

III. Analysis of deformation

A. Analysis of slip

1) Determination of slip plane and slip direction

2) Determination of critical resolved shear stress

B. Analysis of twins

1) Determination of twin planes

2) Determination of other twin indices

a) Vector analysis using goniometric data

b) Vector analysis using metallographic data

c) Stereographic analysis using goniometric data

3) Miscellaneous observations on twinning

a) Relative size versus uniform shear component

b) Lack of annealing twins

The plan of work may be considered to be divided into three phases.

First is the preparation of good quality zirconium crystals large enough to yield quantitative information on the stresses present in slip and twinning. Included here are such problems as determination of geometry and fabrication of desired sample shapes.

Second is the deformation of the zirconium crystals under known conditions, in apparatus suitable for quantitative studies. This phase required building special equipment for compression testing and the modification of existing tensile apparatus.

Third is the analysis of the slip and twinning systems operative in the deformed crystals. This phase includes use of vector analysis methods for the determination of twin indices as well as application of conventional stereographic analysis to this problem.

IV. Description of Material and Apparatus

A. Material

The zirconium used was of two types: (1) as deposited crystal bar zirconium, and (2) arc-melted and forged crystal bar. Chemical and spectrographic analyses of these materials were made, and Table IV shows typical results. All zirconium used was Westinghouse Grade I material, low in hafnium content.

The tantalum foil used to wrap samples was quite pure, as was the fused silica used as container material.

B. Apparatus

1) Apparatus for Annealing and Heat Treating

Three furnaces with controllers, and a vacuum system were the major apparatus used in heat treatment of the samples. Two of the furnaces were Hevi-Duty Electric Co. furnaces type M-2018-8, chromel wound. These two furnaces used in conjunction with Minneapolis-Honeywell regulators model 105C4PS-13 gave a temperature stability of one or two degrees centigrade for long periods of time. A zone six inches long, uniform to two degrees centigrade, was obtained in these furnaces by the use of a stainless steel muffle and careful adjustment of power in each of the three heating zones.

The third furnace was platinum wound and was used to attain temperatures beyond the range of the Hevi-Duty furnaces. The platinum wound furnace had a four inch zone

Table IV: Typical chemical and spectrographic analysis of zirconium crystal bar and arc-melted zirconium crystal bar.

Element	Content in Arc Melted Zirconium Crystal Bar (parts per million, by weight)	Content in Crystal Bar Zirconium (parts per million, by weight)
Oxygen	190	235
Nitrogen	6	5
Carbon	30	110
Hydrogen	46	40
Aluminum	20	40
Calcium	30	30
Chromium	30	30
Copper	25	20
Iron	75	220
Magnesium	8	6
Manganese	6	5
Molybdenum	10	10
Nickel	30	40
Lead	9	10
Silicon	30	20
Tin	15	8
Titanium	20	20
Vanadium	20	20

Note: Carbon found by combustion.

Oxygen found by hydrogen chloride volatilization method in which oxygen is left as zirconium oxide.

Hydrogen found by vacuum fusion techniques.

Nitrogen found by a micro-Kjeldahl process after solution in hydrofluoric acid.

Metallic elements found by emission spectroscopy.

uniform to five degrees centigrade. This furnace was regulated by a Wheelco controller giving a variation of plus or minus five degrees centigrade at 1200° C.

The vacuum system was mounted on a movable table and was capable of producing a vacuum of 5×10^{-7} mm. of mercury. The diffusion pump was an Eimac Diffusion Pump, Type HV-1, and was backed up by a Welsh mechanical pump. Two vacuum gauges were mounted in the system: a Philips Gauge, and an ionization gauge.

The temperatures were measured with calibrated chromel-alumel and platinum-platinum, ten percent rhodium thermocouples. The voltages were read on a Brown Portable Potentiometer, model 126W3, which was calibrated against an Eppley Standard Cell, No. 100, by the use of a type B, Rubicon Potentiometer.

2) Apparatus for Determination of Sample Geometry

The gross geometry of the samples was found by the use of a Wilder optical comparator, and two machinists squares, one six inch size and one three inch size. Auxiliary equipment such as a level and protractor were also used.

The ends of the samples were made flat and parallel by the use of the jig shown in Figure 1. This jig positioned the sample quite accurately, so that very good end geometry was attained.

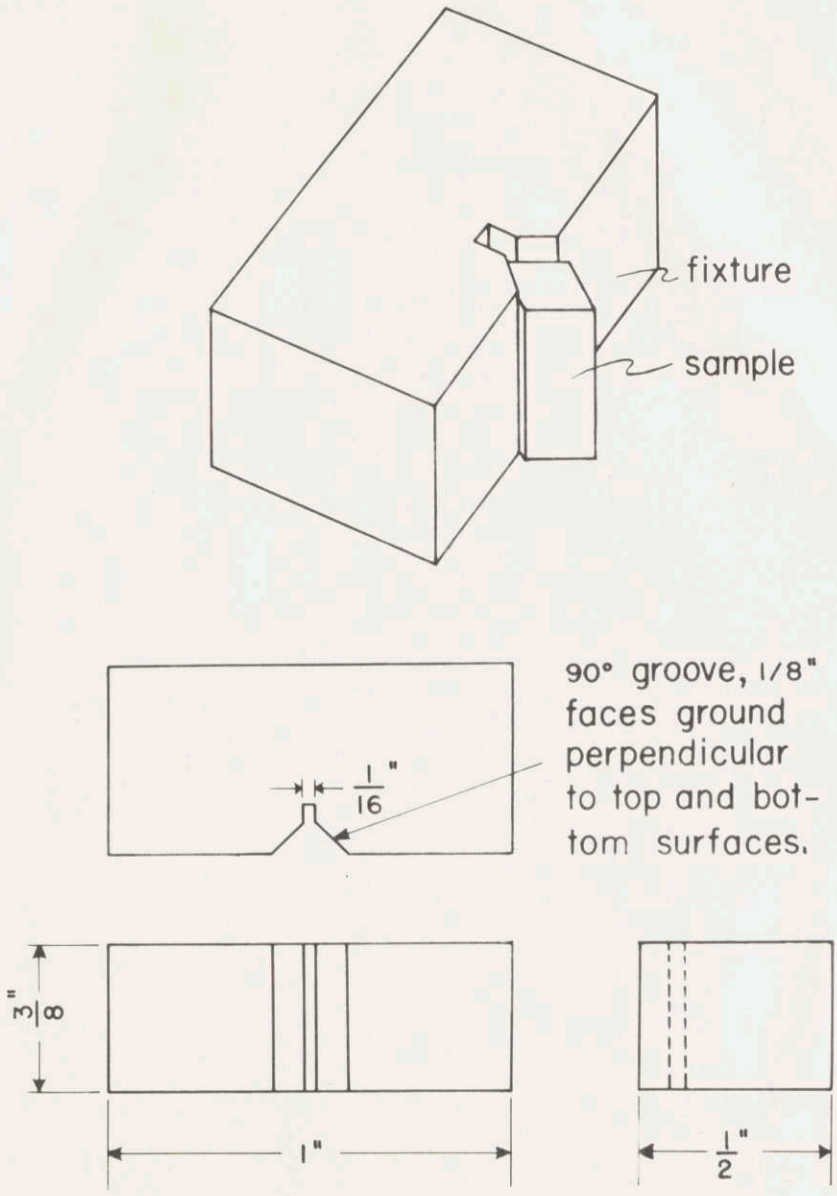

Fig. 1. Fixture used to make ends of compression samples parallel to one another, and also perpendicular to one edge of the sample.

3) Equipment for Crystal Orientation Determination

Laue back reflection photographs of the zirconium crystals were taken on a Unicam S.25 Single Crystal Oscillation Goniometer. This apparatus is shown in Figure 2. A Philips X-ray Diffraction Unit, model 5001, was used as a voltage source for most of the photographs. A Philips molybdenum target tube, model 32113, was used in conjunction with the diffraction unit.

4) Apparatus for Deformation of Samples

Two types of tensile apparatus were used. These are shown in Figure 3 and Figure 4. The apparatus shown in Figure 3 allowed a known increment of strain to be put on a sample within the tensile grips. This was done by turning the large knurled nut at the top of the apparatus which in turn pulled a shaft connected to the movable pair of tensile jaws. This apparatus was very carefully machined so that the shaft connection to the movable jaw had only about one-thousandth of an inch of free play.

The compression apparatus used is given in Figure 5, Figure 6, Figure 7, and Figure 8. One of the compression platens of the apparatus is the flat face of a halved ball-bearing, and the other is the polished end of a micrometer spindle. The half ball-bearing is mounted in a bearing metal and the micrometer spindle rides in a machinist's precision vee-block. The ball-bearing was halved to an accuracy of half a thousandth of an inch by

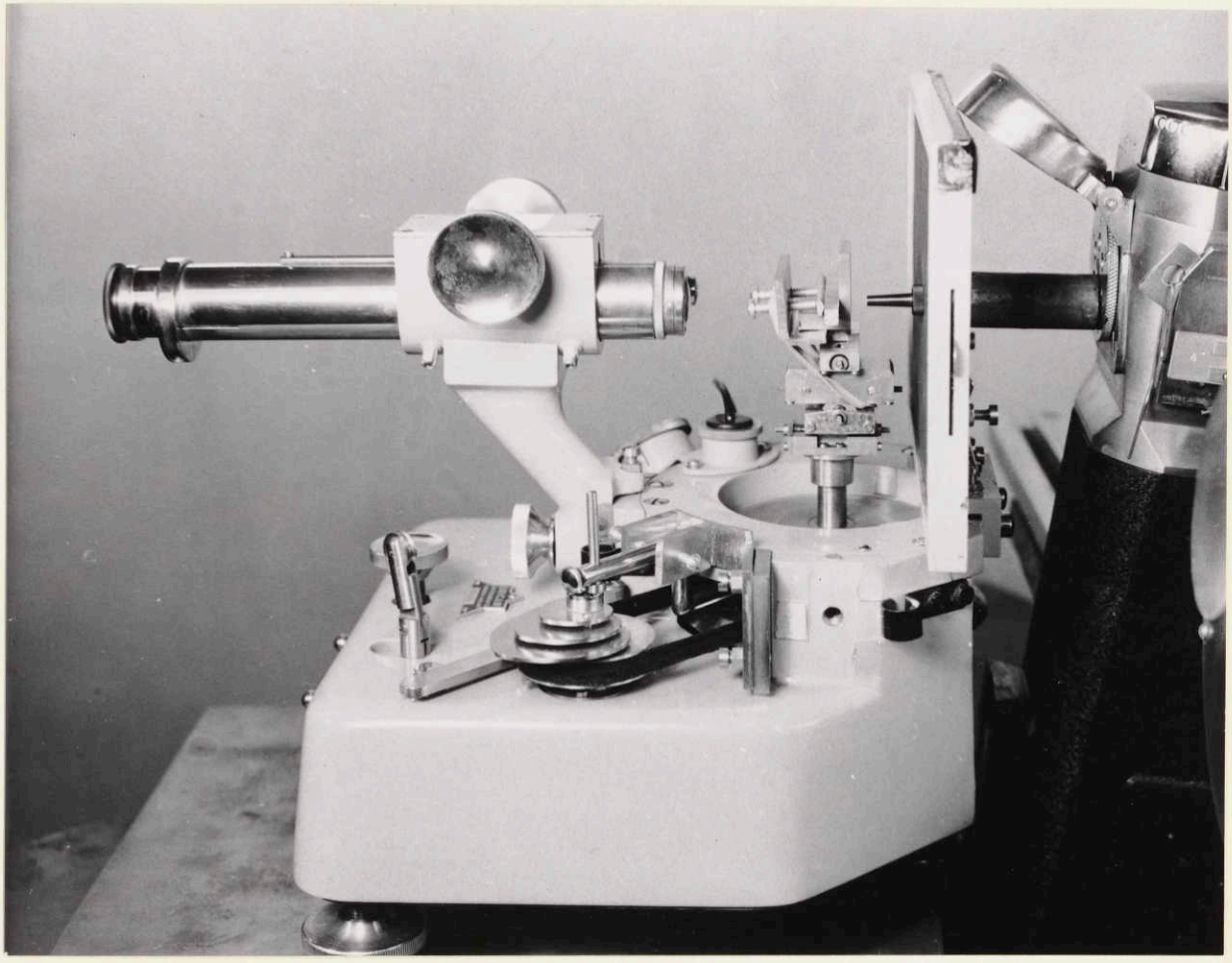

Figure 2: Unicam S.25 Single Crystal Oscillation Goniometer arranged to take Laue back-reflection photographs

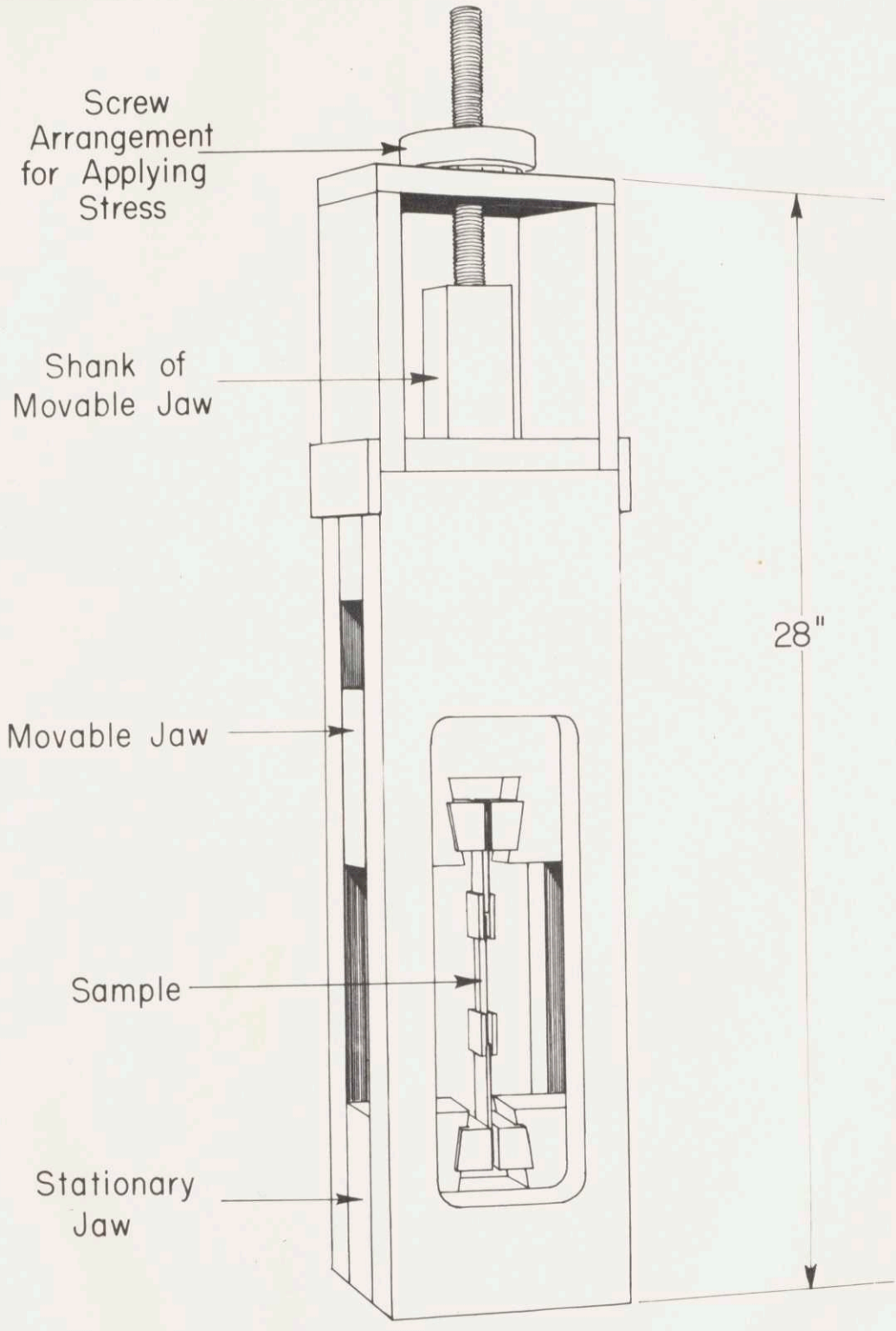

Fig. 3. Diagram of device used for applying tension to zirconium tensile specimens.

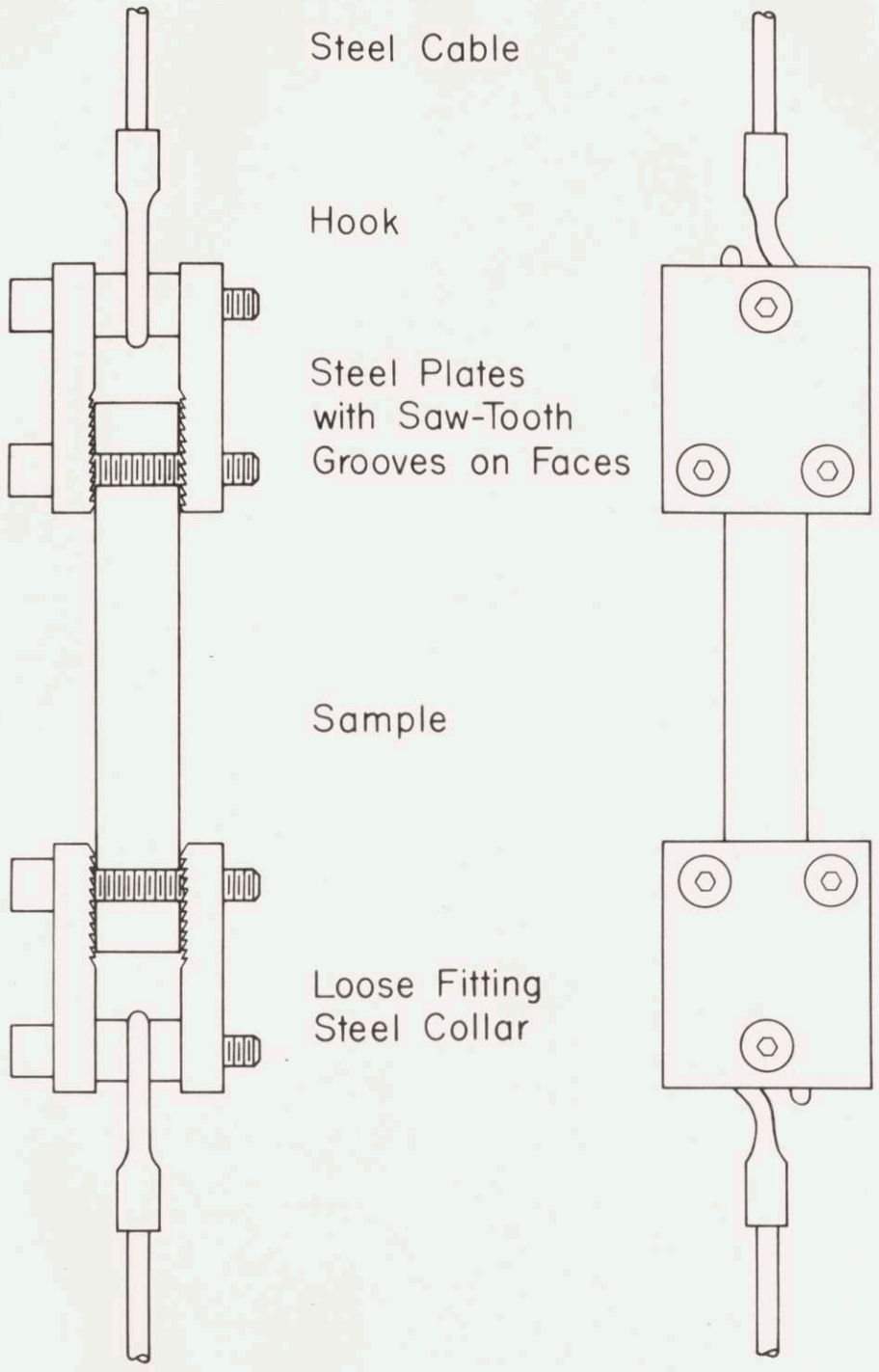

Fig. 4. Tensile grips used for straining zirconium samples.

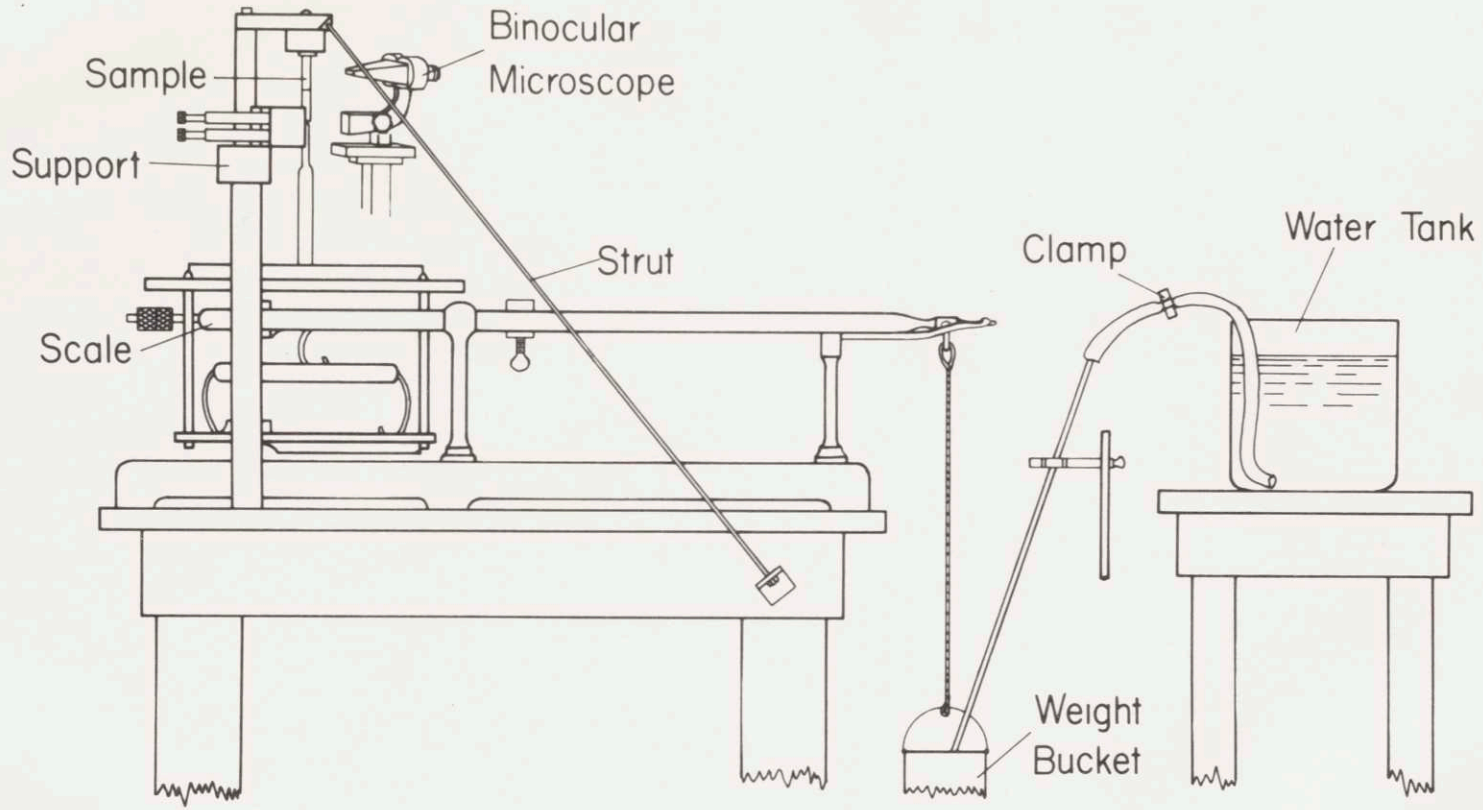

Fig. 5. Schematic diagram of compression apparatus used to deform single crystals of zirconium.

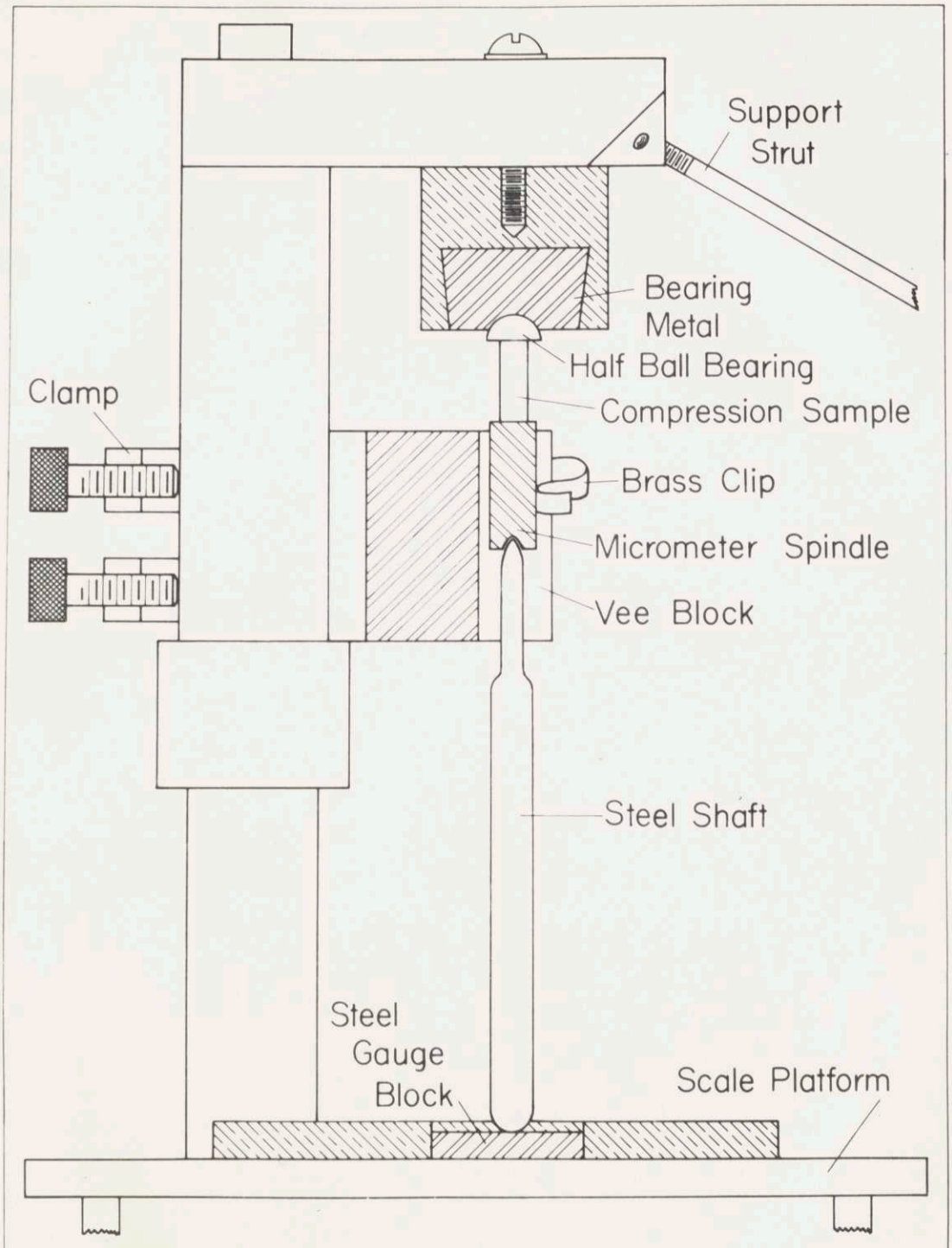

Fig. 6. Schematic section drawing of the head assembly of the compression apparatus used to deform zirconium single crystals.

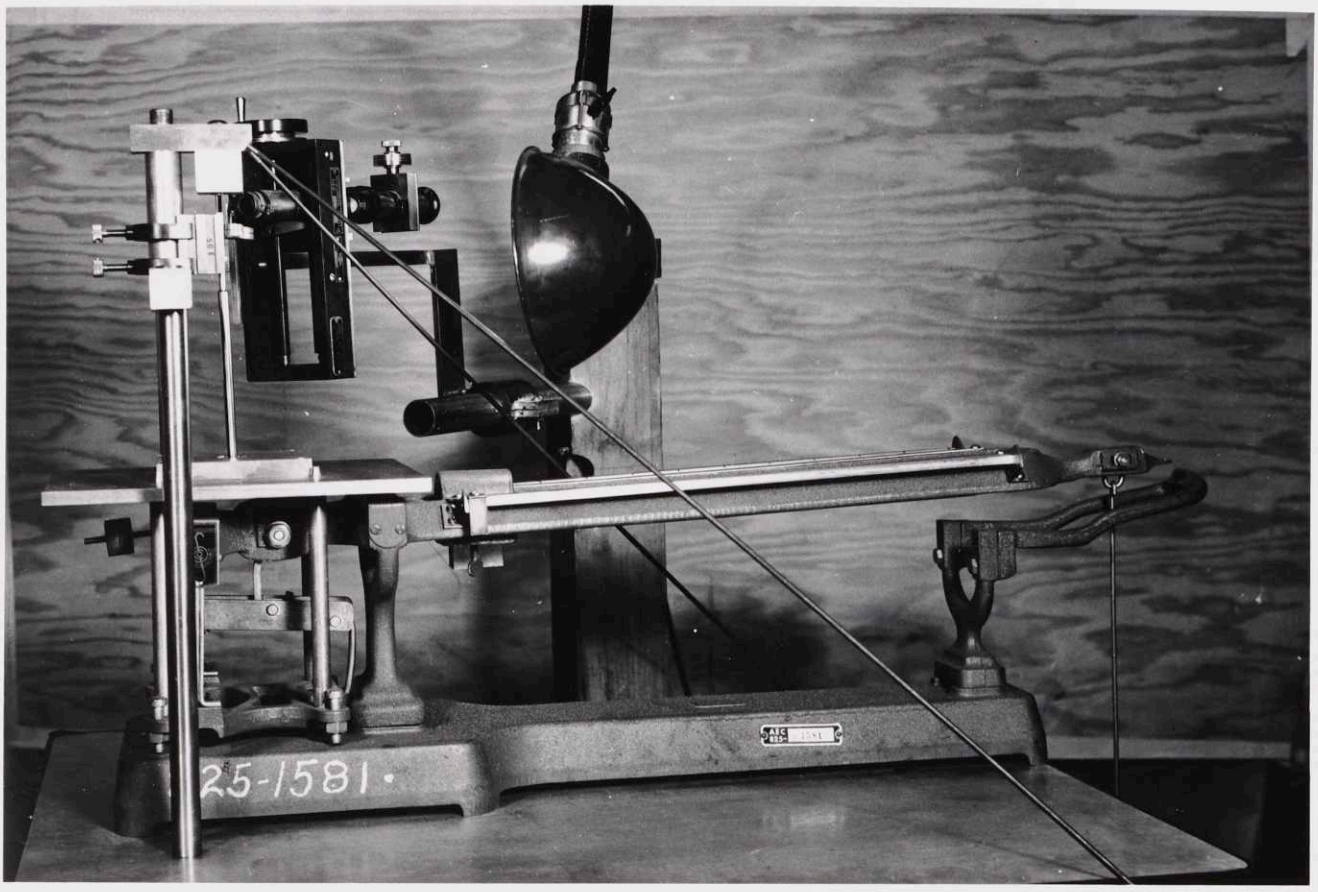

Figure 7: Photograph of compression apparatus used to deform single crystals of zirconium.

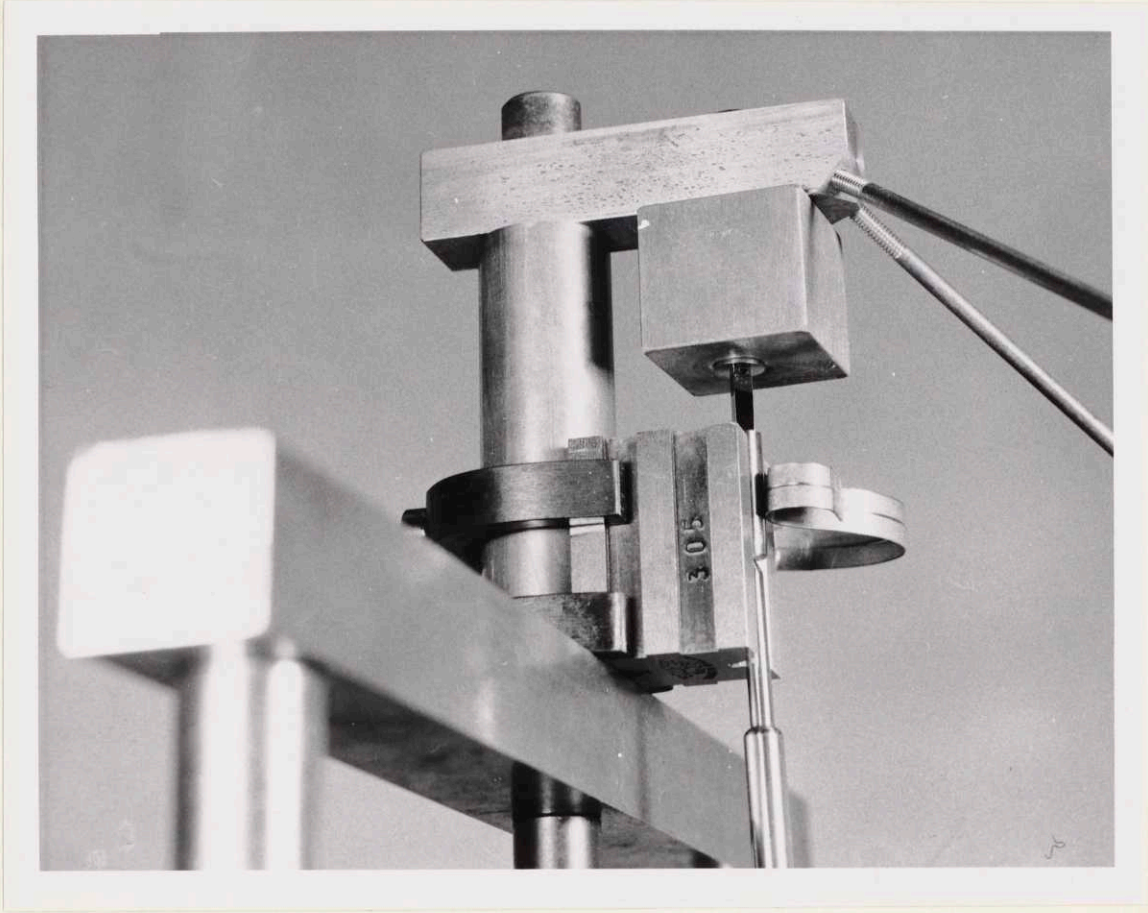

Figure 8: Photograph of the head assembly of the compression apparatus used to deform single crystals of zirconium.

grinding, and then a metallographic polish was given it. The compressive force was obtained by siphoning water into a bucket at the weight pan of the scale. The force was transmitted to the sample by a pusher rod poised between the pan of the scale and the base of the micrometer spindle. A microscope was mounted to focus on the surface of the sample for investigation of the surface as the sample was deformed.

This apparatus was designed to enable compressive forces to be accurately determined and to minimize bending moments in the sample. The frictional resistance of the micrometer spindle against the vee-block was measured and found to be negligible; thus, the compressive load was obtained with good accuracy. Great care was taken to seat the halved ball-bearing so that it would turn under very small eccentric loads. Care was also taken to insure that the flat face of the ball-bearing was very nearly plane, so that even contact might be established with the surface of the compression sample.

5) Apparatus for Examination of Deformed Samples

The deformation markings were examined on a Bausch and Lomb Research Metallograph. The circular revolving stage on this model made it particularly useful for the determination of the angles of deformation markings, as it had a vernier marked to read rotation to one tenth of a degree.

A Bausch and Lomb calibrated eyepiece was also used on the metallograph as a check on the measurement of the angles made by the deformation markings. This instrument had an accuracy of about one fourth of a degree.

V. Report of Work Performed

A. Preparation of Samples

The samples were made of Westinghouse Grade I, low hafnium, crystal bar zirconium. Some crystals were made directly from the crystal bar by heat treatment, and some were made from arc-melted and forged material. See Table IV for typical analyses of the material used.

The first step in the growing of the zirconium crystals was to machine the samples to size. They were then hand polished and chemically etched several times, and given an electropolish. A suitable heat treatment was then employed to grow the crystals, and the crystals were fashioned into test specimens. These steps are given below in detail.

1. Preparation of Crystal Bar Samples

The zirconium was machined into rectangular parallelepipeds about 0.2 inch on a side and two inches long. The last step in the machining was a grinding operation, yielding a good surface and a sample of known external geometry. The samples were then hand polished on emery paper through 3/0 grade, and given a chemical etch followed by repolishing on 3/0 emergy paper. The chemical etch used was a solution of 50 percent distilled water, 45 percent concentrated nitric acid, and 5 percent hydrofluoric acid, by volume.

The geometry of the parallelepipeds was maintained by frequent measurement of thickness at various points on the

lengths. After the second hand polishing the samples were given an electropolish in a bath containing five parts acetic acid to one part perchloric acid, by volume. The cathode used was titanium sheet, and the applied voltage was about sixty volts.

After electropolishing, the samples were washed carefully with soap and water, rinsed in distilled water, then rinsed with pure acetone. They were then wrapped in cleaned tantalum foil and inserted into a clean quartz tube about three feet long, sealed at one end. Acetone was poured into the tube and the samples were again carefully rinsed. In this operation the end of the tube was placed in hot water so that the acetone would boil and insure thorough cleansing of the samples. Most of the acetone was poured off, and the acetone remaining in the tube was removed with a mechanical vacuum pump.

The open end of the quartz tube was then connected to the vacuum system and a vacuum drawn on the samples. The tube was flamed and sparked to attain a good vacuum, and after the vacuum system had run for several days, the pressure was less than 10^{-6} mm of mercury. The movable vacuum system was then positioned so that the end of the quartz tube containing the samples lay inside a muffle furnace initially at room temperature.

The temperature of the furnace was raised at a slow rate (about 200° C per day) so that adsorbed gases might be

driven from the samples and from the tube walls into the vacuum system. The temperature was raised to the equilibrium value of 840° C slowly enough to maintain the pressure below 10^{-5} mm of mercury at all times. The samples were held at 840° C for about ten days. This heat treatment markedly reduced the hydrogen content of the samples and yielded some fairly large grains in the crystal bar zirconium.

Some samples of the crystal bar zirconium and the arc-melted zirconium were analyzed for hydrogen before and after the above heat treatment. These analyses yielded the following results:

a) Crystal bar zirconium: the hydrogen content before annealing was forty parts per million by weight, and after annealing it was two parts per million.

b) Arc-melted and forged crystal bar: the hydrogen content before was forty-six parts per million by weight, and after annealing it was one part per million.

These samples were analyzed at Battelle Memorial Institute by dissolving the samples in an iron bath at 1600° C and analyzing the evolved gases for hydrogen by the low pressure, fractional freezing method. The sensitivity of the apparatus used is equivalent to about plus or minus 0.5 part per million of hydrogen for the two gram sample submitted.

Zirconium seems to form a hydride with even very small amounts of hydrogen present, and this hydride appears as a second phase in the microstructure and changes the deformation characteristics (Schwartz and Mallett, 1953). A photomicrograph of the typical structure of zirconium before hydrogen removal is given along with a photomicrograph of the structure after annealing in Figure 9.

Samples of zirconium were also analyzed for silicon, oxygen, and nitrogen before and after annealing to determine the extent of pick-up of these elements. It was expected that these would be the major impurities introduced in the annealing process. It was found that the impurity level of these elements remained quite close to that given in the initial analysis (Table IV). A typical analysis of the final level of these elements was found to be about two hundred parts per million of oxygen, ten parts per million of nitrogen, and fifteen parts per million of silicon, for samples treated as described above.

The soaking temperature of 840° C given above was chosen because it was reasonably close to the alpha-beta transformation temperature of zirconium. This transformation occurs at about 865° C (Burgers, 1934, p. 563). Samples cycled through this transformation have rumpled and corrugated surfaces. Therefore, it was desirable to keep the samples below the transformation temperature

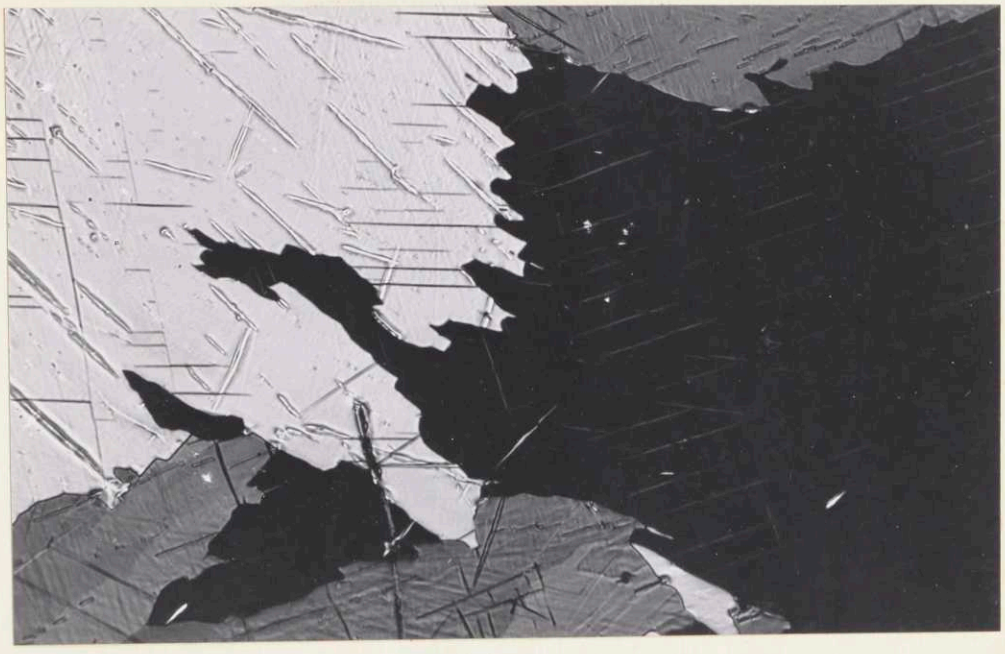

(A)

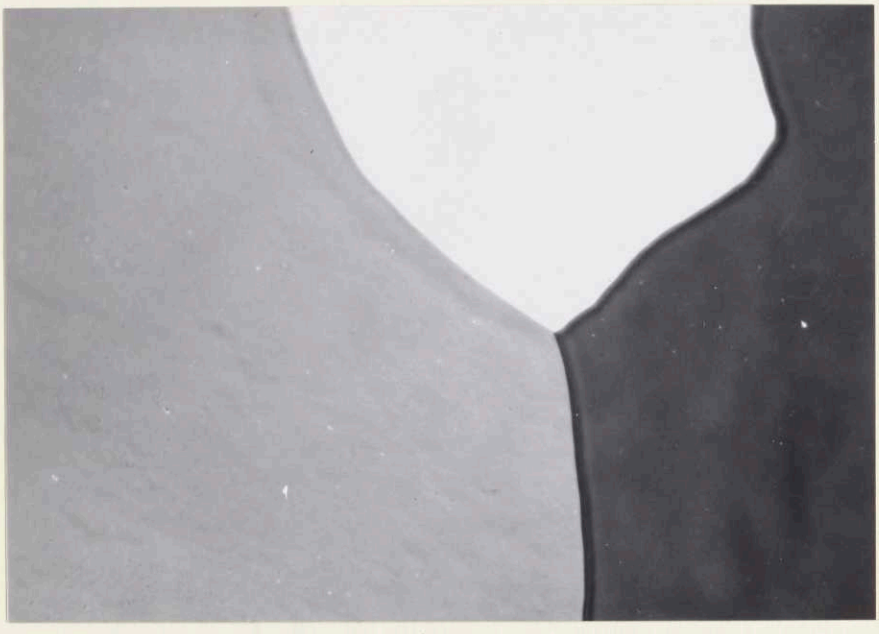

(B)

Figure 9: (A) Photomicrograph of crystal bar zirconium before hydrogen removal. 150x, polarized light.

(B) Photomicrograph of crystal bar zirconium after hydrogen removal. 150x, polarized light.

even though the hydrogen might be removed more quickly at temperatures above the transformation.

Some of the grains produced by the above treatment covered the entire cross-section of the sample and grew to lengths of one-half inch. Grains produced in this manner had smooth surfaces and required no paper polishing after the annealing. Judged by the sharpness of the spots on the Laue back reflection photographs, and from the appearance of the grains under polarized light in the metallograph, the crystals were of good quality. This method gave a yield of about one good sample for every twelve or fifteen treated. A photograph of a good sample produced in this fashion is given in Figure 10.

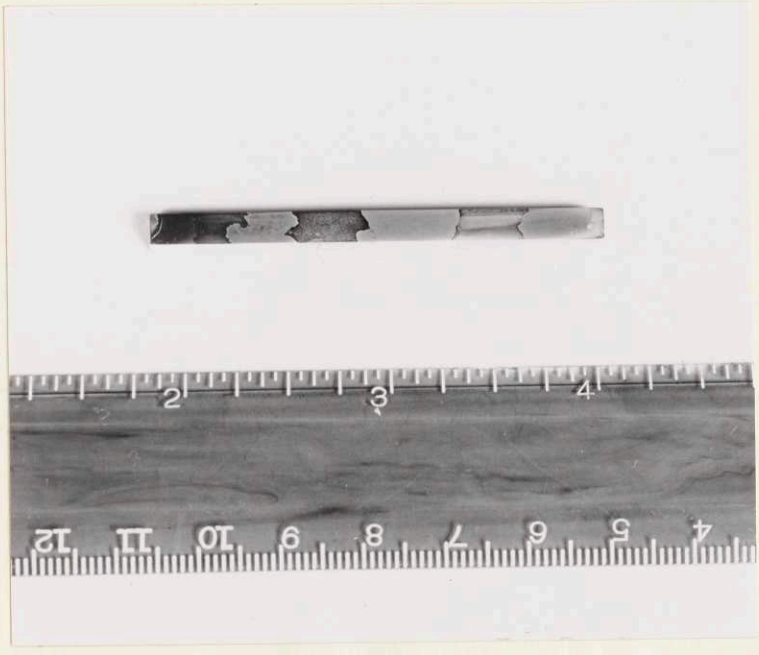

Figure 10: Photograph of large grains produced in a sample of crystal bar zirconium by a long anneal at elevated temperature.

One of the main troubles with this method, so far as this work was concerned, was that the crystals produced all had roughly the same orientation with respect to the sample axis. The basal planes of the samples were all within eighteen degrees of being parallel to the sample axis. Another poor feature of the crystal bar was that it had growth flaws, such as cracks and crevices, and these could make it difficult to obtain values of critical resolved shear stress for slip.

The particular preferred orientation observed in these samples might be expected if one assumed the large crystals to be formed by simple grain growth. The reason for this expectation is that the crystal bar zirconium, as grown, has this same preferred orientation (Burgers, 1934, pp. 564-569).

At least one other investigation has yielded fairly coarse crystals of zirconium by methods basically the same as that given above (Brick, Lee, and Greenewald, 1950, p. 3). However, these particular samples seemed to contain the zirconium hydride phase which presumably prevented the growth of larger crystals.

2. Preparation of Arc-Melted Samples

The initial steps in making large crystals of the arc-melted and forged zirconium was the same as that given above for the crystal bar samples. Samples of the arc-melted material received the same machining, cleaning, and annealing treatment. They were then examined for large

grains, and those that did not have large grains were given an additional heat treatment.

This heat treatment was basically a cycle above and below the alpha-beta transformation temperature, repeated several times. This was essentially the method used by one group of investigators to make large crystals of titanium (Anderson, Jillson, and Dunbar, 1953, pp. 1191-1192).

The zirconium samples that were to be heat treated by cycling were re-wrapped in tantalum foil after thorough cleansing, and sealed in a quartz container at a pressure below 10^{-6} mm of mercury. These samples were then annealed at 1200° C for four hours and then quickly transferred to a second furnace set at 840° C and allowed to remain at the lower temperature for five to ten days. At the end of the lower temperature anneal, the samples were transferred back to 1200° C furnace, and the whole cycle repeated once or twice more to complete the treatment. At the end of the last hold at 840° C the furnace temperature was dropped to room temperature at a rate of about one hundred degrees centigrade per hour to avoid stressing the samples. When the furnace reached room temperature, the sealed containers were opened by breaking the ends in a vise. This method of opening insured that very little damage was done to the samples.

After cycling, the quartz tubes generally had a thin flaky coating inside, but the zirconium and tantalum were quite bright. A typical silicon content after cycling was about fifteen parts per million, the oxygen was about two hundred parts per million, and the nitrogen content about ten parts per million. This analysis may be compared with that of the untreated material as given in Table IV to show that there was very little contamination during the heat treatment. The tantalum foil tended to stick to the zirconium samples at the edges but the wrapping was generally pried off with no difficulty.

The surface of the samples after this treatment was rough and rumpled. A photograph of such a sample is shown in Figure 11. It was necessary to repolish these samples on emery paper to obtain rectangular cross-sections and plane faces. Accordingly, the samples were very carefully polished by hand on kerosene lubricated emery paper through 3/0 paper. They were then given a chemical etch in the nitric acid-hydrofluoric acid solution described above, and repolished on 3/0 and 4/0 emery papers. The samples were given an electropolish at this point and were inspected metallographically. Those crystals large enough to use in deformation studies were set aside.

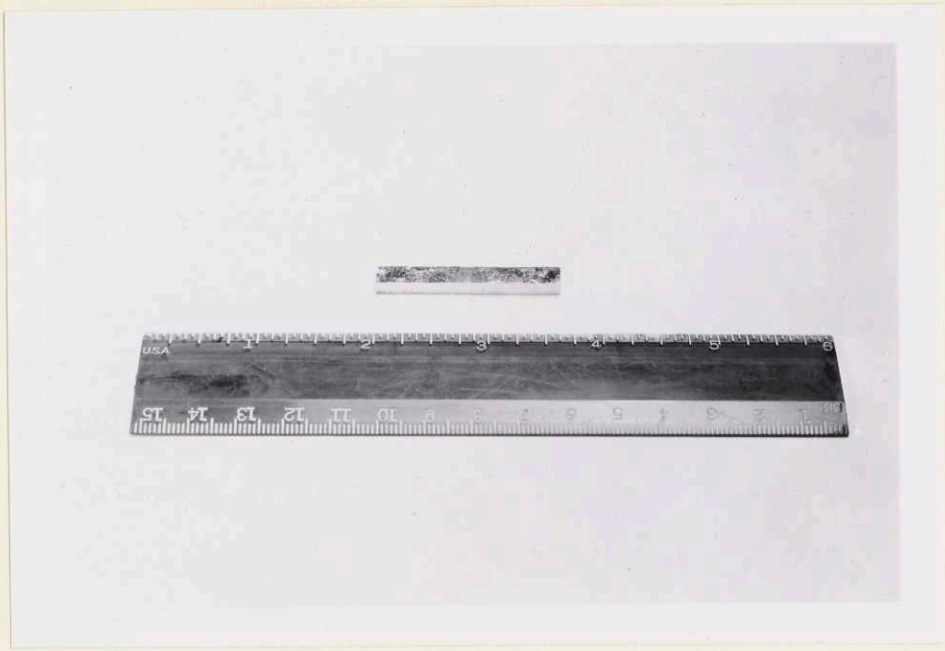

Figure 11: Photograph of a zirconium sample cycled several times through the alpha-beta transformation temperature.

The usable crystals obtained in this manner covered the entire cross-section of the rod and were up to three-quarters of an inch long. It was found that these grains were produced with a more random orientation than grains grown in crystal bar, and the orientations ranged throughout the stereographic triangle.

A stereographic triangle is given in Figure 12 in which is plotted the axes of all the samples tested. The point plotted represents, for each sample, the direction of the tension or compression axis with respect to the crystallographic poles at the corners of the triangle.

The crystals produced by this method gave sharp spots on Laue back reflection photographs, and looked quite

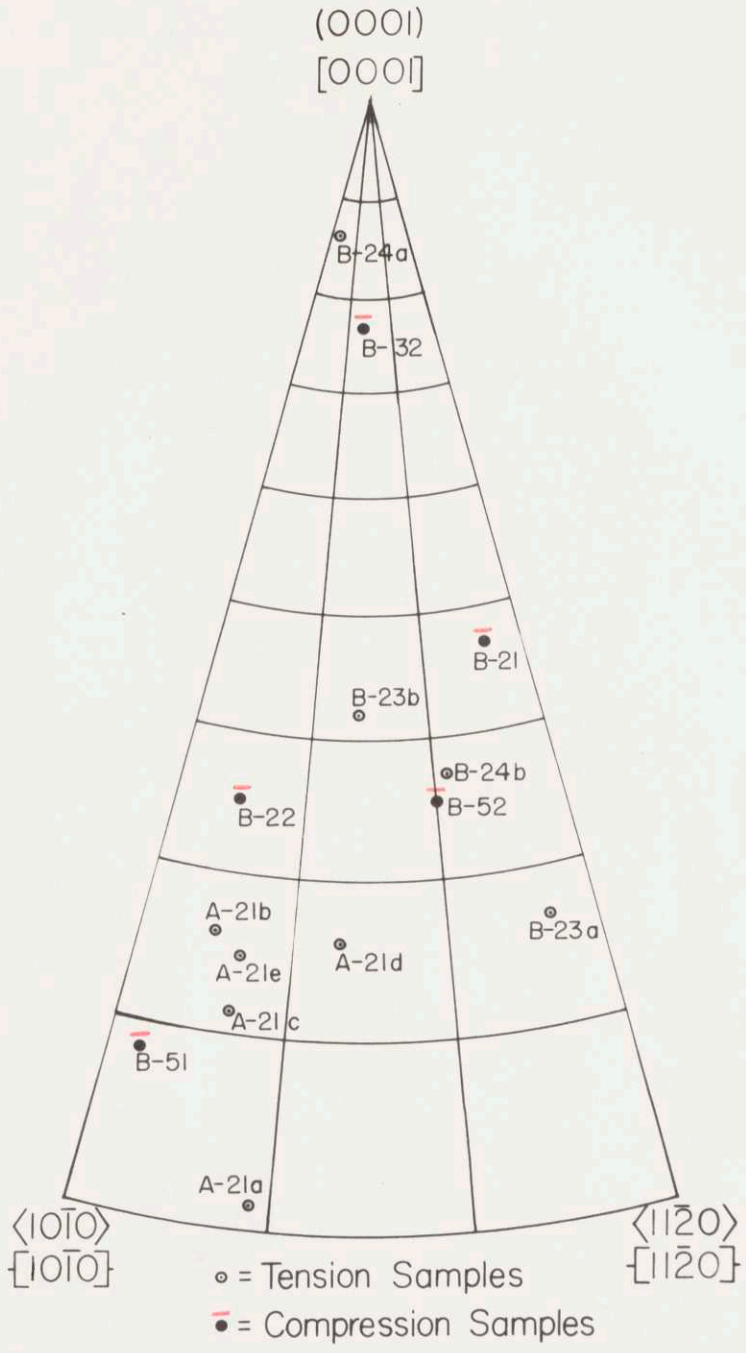

Fig. 12. Orientations of crystals of zirconium used in deformation study. Points indicate stereographic projections of specimen axes.

uniform under polarized light when examined metallographically. A typical Laue photograph, representative of crystals produced this way as well as by simple soaking, is shown in Figure 13.

In addition to the methods detailed above, several other processes of obtaining single or coarse crystals were tried. The strain-anneal method was tried with no success. Luetzow (1950) has made a study of the critical strain of zirconium and has made crystals up to about four millimeters in diameter. Churchman (1954), however, has been quite successful in using the strain-anneal technique to make large crystals of titanium.

Another unsuccessful experiment that was tried was to cool the samples very slowly from 1200° C through the transformation temperature. This was done by two methods: one was to lower the temperature of the furnace containing the samples, and the other was to slowly lower the samples, suitably sealed in quartz, from a 1200° C zone in a furnace through a gradient into a cool zone. A good deal of experimentation was devoted to these methods, but they were not successful.

3. Selection and Preparation of Tensile and Compression Samples

The crystals made by the above methods were examined and it was decided whether a given bar was to be retained as a tensile specimen, cut into compression samples, or

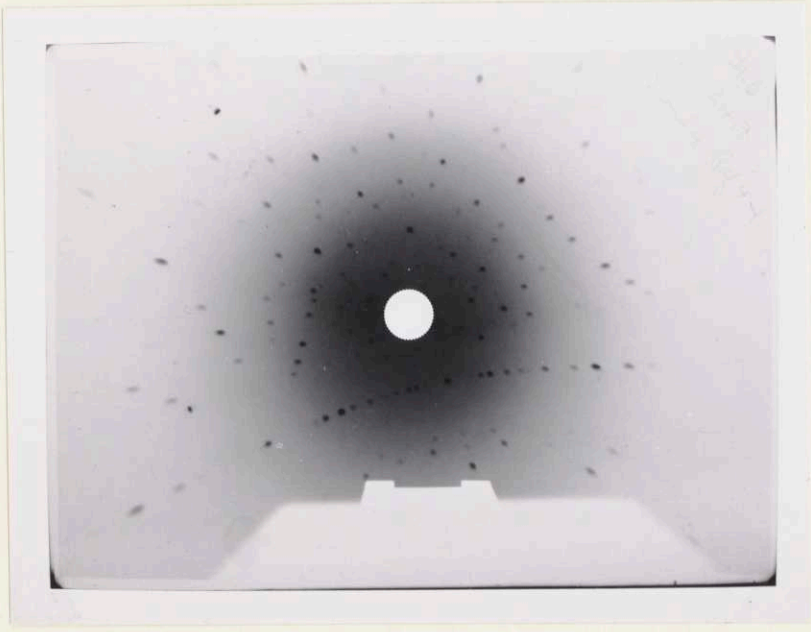

Figure 13: Laue back reflection photograph of a zirconium crystal. Unfiltered molybdenum radiation, 40 kilovolts, 8 milliamperes, and 90 minute exposure. (Reduced to approximately one-half actual size.)

recycled. In good crystals the factors that influenced the decision were such things as the location and size of the usable crystal within the bar and the presence of other usable crystals in the same bar. For those bars containing several crystals to be tested in tension, maps of the surface traces of the grain boundaries were made. These maps were made with the aid of an optical comparator at twenty times magnification so that faithful reproduction was obtained. The tracing was then useful for grain identification and for keeping the geometry and Laue photographs in good order.

Samples that had only one large crystal in them, with that crystal at one end of the sample, were cut to make compression specimens. Also cut into compression specimens were samples with several long crystals, or samples which, when sectioned, would give a larger number of useful crystals.

The samples were mounted and cut quite carefully to insure minimum damage to the crystals. The samples to be cut were first glued to flat bars of steel. The steel could then be gripped in a vise without stressing the sample. A bar with a sample glued to it was then aligned under an abrasive cut-off wheel and the cuts were made. A coolant was used and the cuts were made very slowly and with extreme care. The cutting process generally caused mild twinning of the crystal on the cut surface; however,

these twins extended only a few thousandths of an inch into the crystal and were easily polished off on emery paper.

The cut ends of the crystals were made flat and parallel to one another by the use of the fixture shown in Figure 1. This fixture positioned the samples so that on each sample the two ends were made flat and also perpendicular to one edge of the sample. The fixture was made from a machinist's parallel and has a 90° groove ground in one face. This groove is perpendicular to the two faces it intersects, and it has a slit at its vertex to accommodate the edges of samples that vary from a perfect fit.

The sample is placed in this fixture and held in position with one's finger. The fixture and sample are then pushed across a sheet of emery paper to effect the polishing of one end. The device is pushed in one direction only, and when one end is finished the sample is turned about so that the opposite end is positioned to be polished. One ought to have the same faces of the sample against the fixture for each of the two ends polished, so that the two ends will be perpendicular to the same edge of the sample.

Samples ground in this jig had ends that gave the same micrometer readings on the four corners to within one ten-thousandth of an inch. The ends were perpendicular to the two faces which lay against the fixture, as was

evidenced by closing out light in the right angle of a machinist's square. These ends were also quite smooth as they were polished through 4/0 emery paper. Thus, with this fixture, samples were made that had good end geometry for compression testing.

4. Measurement of Angles Between Faces of the Specimens

The dihedral angles between adjacent faces of each of the samples were measured. These angles were important because they were necessary in obtaining the twin and slip indices, and they were also necessary in one method of calculating the cross-sectional area of the specimens.

Figure 14 illustrates the method used to measure the dihedral angles between the faces of the samples. A sample, whose cross-section is represented by abcd, was placed on a plane piece of paper, and, by standing the sample in some clay, was positioned so that faces ab and cb were perpendicular to the plane of the paper. This was done by the use of a three inch machinist's square. Pins were placed at positions I and II and were made normal to the plane of the paper. The reflection of these pins off surface ab was sighted in a thin slit placed normal to the plane of the paper. A mark was made at four or five points where the observer saw the two pins aligned as one. The line determined by these marks, ON in Figure 14, is the reflected direction of the beam determined by I and II. The line OM, bisecting the angle made by the incident and reflected

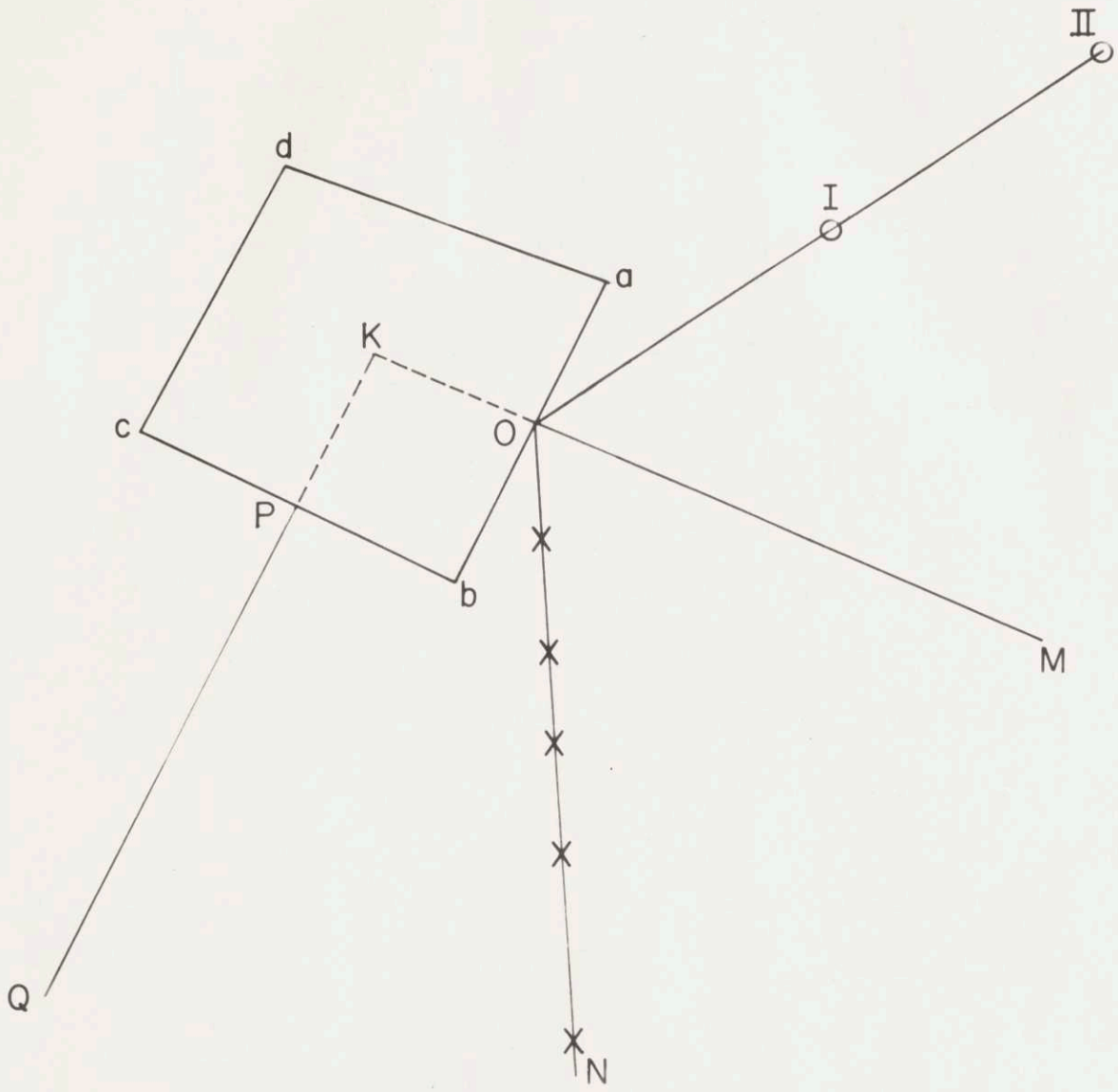

Fig. 14. Optical method of obtaining the dihedral angle between two planes.

beam, is normal to the plane of face ab.

A similar set of operations is performed on the adjacent face, bc, to determine the normal PQ. The angle between the faces ab and bc is then found by extending QP and MO to intersect at K, yielding the angle OKP. This angle is the supplement of the angle ObP, the angle between the two adjacent faces.

If the sample has plane faces and a uniform cross-section, one may find all four dihedral angles without changing the initial position of the specimen. Careful polishing of the specimens insured this condition. If this condition were not met, one would align the two faces of interest and obtain the dihedral angle between these two faces. Then, upon going to the next pair of faces, one would realign the sample so that the second pair of faces was perpendicular to the plane of the paper. Thus, a determination of all four angles could be made.

An additional method for determination of the dihedral angles between faces was used on the compression samples. This method consisted of measuring the angles directly by using an optical comparator to project the end of the sample onto a viewer. Angles measured in this manner agreed with those measured by the other method to within plus or minus half a degree, generally, and always within one degree. This second method also provided a convenient method of measuring the cross-sectional area of the

compression samples, since the entire cross-section was magnified twenty times on the viewer of the optical comparator. Traces were made from the image on the viewer, and the measurements made from these traces.

5. Preparation and Analysis of Laue Photographs of Crystals

Back reflection Laue photographs were made of each crystal to determine the crystal orientation. These photographs were made on a Unicam S.25 Single Crystal Oscillation Goniometer. This equipment is shown in Figure 2 with a sample in place.

Particular care was taken in the alignment of the apparatus to ensure accurate determination of crystal orientation. A specimen holder was made to position the samples so that a face on the sample could be made parallel to the film, and one edge in that face parallel to the edge of the frame of the film holder. The face to be photographed was positioned three centimeters from the film to within one hundredth of a centimeter. All lines and planes that were to be parallel were checked by the use of surface plates, squares, and dial indicators. These lines and planes were all made parallel to tolerances of less than one-tenth of a degree.

It is estimated that the major errors of orientation determination stemmed from film shrinkage and errors in the Greninger chart and the Wulff net. However, these errors are estimated to be under one-half a degree.

On each crystal, Laue photographs were taken on each of three faces. Each set of Laue pictures so taken was plotted on a single stereogram, and the orientation of the crystal determined by the use of standard techniques (Barrett, 1952). The three photographs of a given crystal generally checked with one another to within one degree. In the few cases of error greater than this, the fault lay in misalignment of the sample. In these cases either a new photograph was taken, or the remaining two photographs were accepted as representing the correct orientation. Care was taken to keep the error of the crystal orientation determinations to a minimum because the precision was needed to distinguish among the multiple possibilities of active deformation planes.

The Laue photographs were taken at forty kilovolts across the x-ray tube, and eight milliamperes in the filament. The target material was molybdenum and no filter was used. Exposure times ranged from one hour to one and one-half hours, the latter being the most satisfactory. All the photographs were made either on a Philips X-ray Diffraction Unit or on a Picker Unit.

A typical photograph, exposed for one and one half hours at forty kilovolts and eight milliamperes with a molybdenum target, is shown in Figure 13. Some satisfactory Laue photographs were also made with a copper target at twenty-three kilovolts and thirteen milliamperes, with no filter and a seventy minute exposure.

B. Deformation of Samples

The samples, as prepared and processed above, may be divided into two groups: tensile specimens and compression specimens. A detailed description of the deformation of samples from each of these groups is given below.

1. Deformation of Samples in Tension

a) Strain Measured

Five of the crystals deformed in tension were deformed in the tensile apparatus pictured in Figure 3, which was previously discussed in the section on apparatus. Samples deformed in this apparatus were elongated to specific strains, with no measurement of the stresses involved. The five crystals so tested were A-21a, A-21b, A-21c, A-21d, and A-21e. A single bar containing these five crystals was given an electropolish and then carefully positioned in the tensile grips of the apparatus. The bar was strained 0.55 percent and then examined metallographically to record the strain markings, i.e. the slip and twin traces. The bar was then placed back in the apparatus and strained enough to bring the total strain to 1.4 percent. Again the strain markings were observed metallographically and the traces and general features recorded. The sample was then strained to a total of 2.2 percent and examined. This procedure continued to a total strain of 10.7 percent, with intermediate inspections at 3.7 percent and 6.3 percent.

The five crystals deformed in this manner were prepared from crystal bar zirconium and were made by holding at 840° C as described above under Preparation of Crystal Bar Samples. The orientations of the five crystals described above are given in Figure 12 together with the orientations of the other crystals tested.

b) Stress Measured

Four additional crystals were deformed in tension under conditions of known stress, but unknown strain. These samples were held in grips as shown in Figure 4, and deformed by the action of known loads.

The four crystals deformed in this manner were in two bars, each bar containing two crystals. These crystals are B-23a, B-23b, B-24a, and B-24b, and their orientations are given in Figure 12.

Samples deformed by this method were observed with a microscope while the force was steadily increased. The load was added by allowing water to flow into the load-carrying container.

A microscope was used to observe the first visible evidences of slip or twinning. The load corresponding to these first deformation markings was taken, and the sample examined metallographically to obtain the active planes. The samples were then replaced and the deformation continued until new markings were observed. These were determined as they appeared, and the loads to produce them were noted. The maximum load applied to these crystals was

about ten times that to produce the initial deformation markings.

2. Deformation of Samples in Compression

Five single crystals were made and tested in compression. These samples were tested in compression apparatus shown in detail in Figure 5, Figure 6, Figure 7, and Figure 8. The apparatus is described in the section on Apparatus for Deformation of Samples. These five crystals are B-21, B-22, B-32, B-51, and B-52, and their orientations are given in Figure 12. A photograph of these five crystals is given in Figure 15.

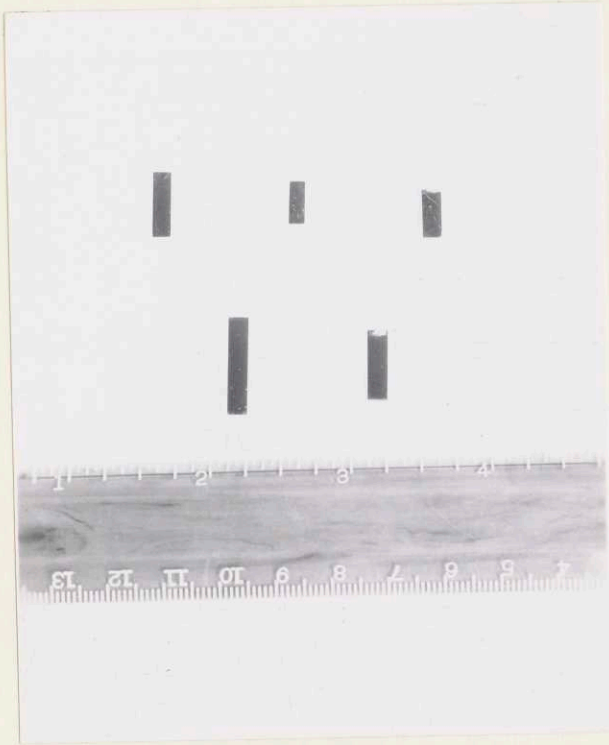

Figure 15: Photograph of five compression samples after testing.

Each of the samples was placed between the compression platens and loaded to produce deformation markings. The samples were observed with a microscope so that the first visible traces of slip or twinning might be noted. The loads applied to give these traces were recorded, and the samples carefully removed and examined in a metallograph. The angles that the traces made with the reference edges were measured and the twin or slip planes obtained as given below in the section on Analysis of Deformation Processes.

After the initial loading and examination, the compression loading was continued to produce more deformation traces. The loads corresponding to these new traces were measured and the traces were examined in a metallograph to determine the active planes and the features of the deformation produced. The progressive loading followed by metallographic examination was continued to loads about three times that required for the initial visible deformation.

C. Analysis of Deformation Processes

1. Analysis of Slip

Slip was observed in all fourteen crystals tested, and in every case it was found to occur on $\{10\bar{1}0\}$ planes. The analysis of the slip elements, the plane of slip and the direction of slip, may be done in several ways. Those used in this work are discussed in the following section.

a) Determination of Slip Plane

1) Determination of Slip Plane by Two Trace Method

Crystals of various orientations (see Figure 12) were pulled or compressed to produce deformation traces. These traces very often were produced on two adjacent faces and intersected at the common edge. An example of this is given in Figure 16 for $\{11\bar{2}2\}$ twinning. If traces on two adjacent faces may be paired without ambiguity, the active plane may be uniquely determined, as the two traces define a plane in the crystal lattice.

The angles that these traces make with the common reference edge are easily obtained using a metallograph with a revolving circular stage and an eyepiece with a reference line in it. With the equipment used it was possible to determine these angles to a maximum accuracy of three minutes of arc. As an additional check, a goniometer attachment was used in one of the eyepieces of the metallograph. This goniometer read the angles to an accuracy of about fifteen minutes of arc.

The deformation traces were examined at various magnifications ranging from twenty diameters to five hundred. Metallographic examination was done in bright field as well as with polarized light.

If one has traces on two adjacent surfaces paired with one another, and desires the crystallographic indices of the active plane, one makes use of a Laue photograph of the crystal and the application of stereographic projection.

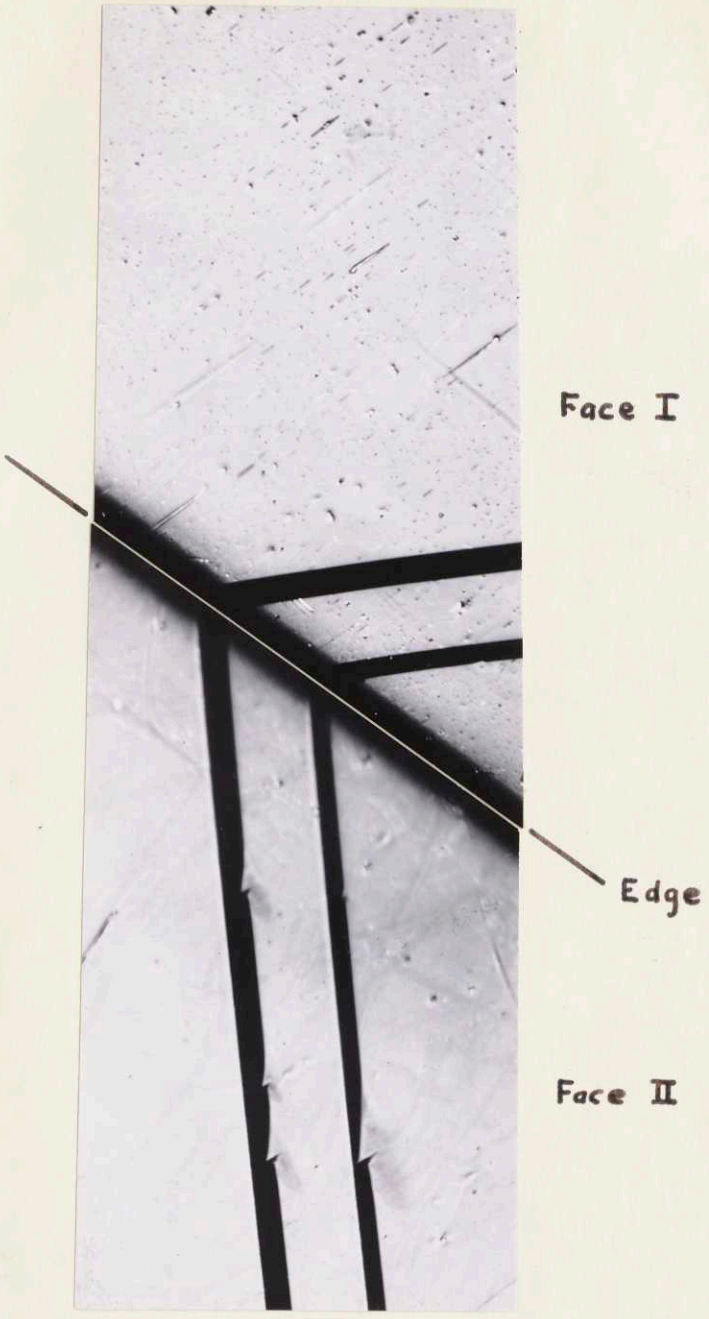

Figure 16: Traces of $\{11\bar{2}2\}$ twins on two adjacent faces of a sample. 175x, polarized light.

This method is fully described in Chapter II of Barrett (1952)

The Laue photograph is first plotted on a stereographic projection of the crystal with the aid of a Greninger chart and a Wulff net. The angle between the slip trace and the common edge is plotted on this same stereogram for each of two intersecting slip traces on two adjacent faces. The plane of the two traces is then defined and its pole easily obtained.

This method is illustrated in Figure 17, parts (A) and (B). The diagram in Figure 17(A)represents a crystal that has slipped (or twinned) producing traces on surfaces I and II. The trace on surface I makes an angle α^{I} with the reference edge NS and the trace on II makes an angle α^{II} with this edge. The dihedral angle between surfaces I and II is given by A.

If a stereographic projection of this crystal is made as in Figure 17(B), one may obtain the pole of the active plane. In this diagram surface I was made the plane of projection. Surface II was plotted on this diagram as a great circle at an angle A from surface I. The reference edge NS is common to both surfaces and is so given in the projection. The angles α^{I} and α^{II} were plotted in the projection on the planes of surface I and surface II as points X and Y. These angles represent two lines of the active plane, and the plane is found by rotating a Wulff net about the projection to obtain the great circle containing both X

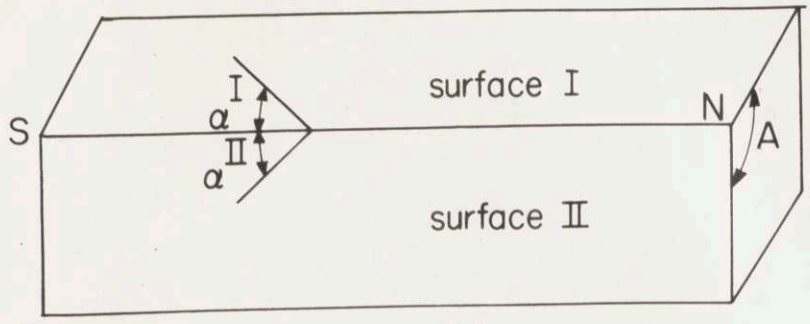

(A)

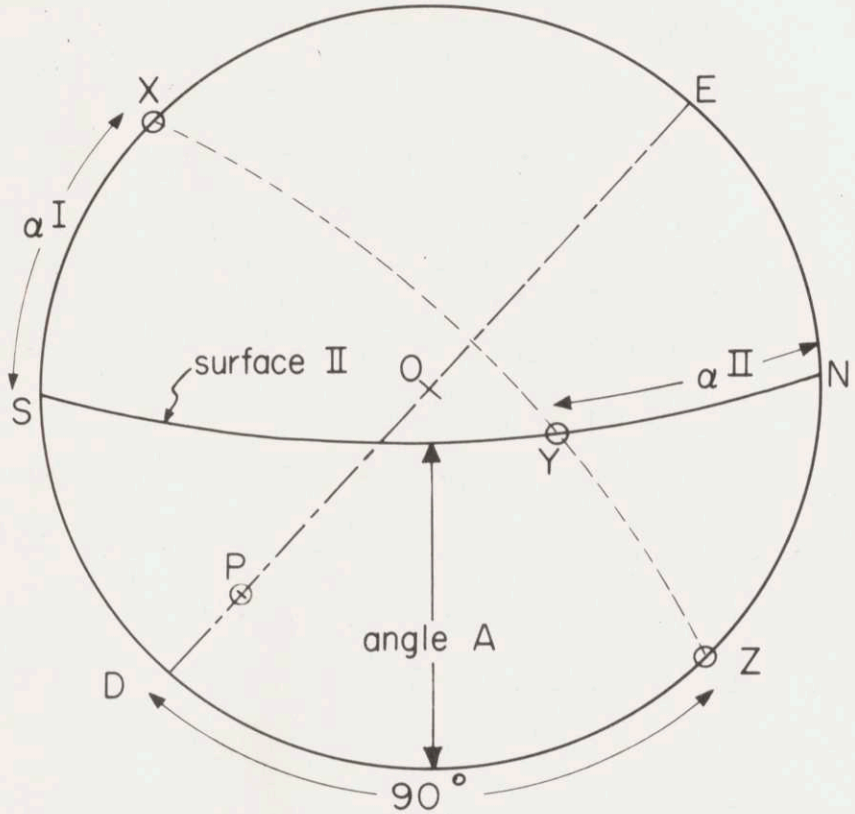

(B)

Fig. 17. (A) Crystal with slip or twin traces on two adjacent faces.

(B) Stereographic solution for pole of active plane. Projection plane is plane of surface I.

and Y. The active plane is this great circle, given as XYZ. The pole of this plane is found at point P and the active plane is then defined.

A Laue photograph of the crystal, suitably plotted on this same stereographic projection, would permit determination of the crystallographic indices of the active plane.

2) Determination of Slip Plane by Single Trace Methods

The use of a single surface trace to determine an active deformation plane is not so definitive as the use of two traces. A single trace defines only the locus of possible positions for the pole of the active plane. This locus is the equatorial great circle of the stereographic projection when the face in question is the projection plane, and the poles of the Wulff net are rotated so that one pole lies at the angle alpha from the reference line. The notation used here is consistent with that used in the section above, and reference is again made to Figure 17.

The locus described above is given graphically in Figure 17. In this figure the great circle DOE is the locus of poles of all planes intersecting surface I to give traces at an angle α^{I} from the reference line NS in the sense drawn in Figure 17.

If one plots a Laue photograph of the deformed crystal on this same stereographic projection, one may determine

those crystallographic poles lying on the great circle DOE. By repeated experiments, or by crystallographic reasoning one may then select the active crystallographic plane.

If many different crystals are to be analyzed by a single trace method, it is often best to refer all the crystals to a standard projection. The great circles given by the loci of possible active poles are also plotted on this standard projection. The loci will then intersect at the pole of the active plane, thus giving a definitive solution from the active plane (Cahn, 1951, p. 9).

In this work very few single trace determinations were made, and those planes so found were all confirmed by the two trace method. The slip planes found by these methods were $\{10\bar{1}0\}$, the prism planes of type I.

b) Determination of Slip Direction

To completely define the slip systems of a metal one needs to specify both the slip planes and the directions of slip in these planes. Generally, the plane of slip is the crystallographic plane of densest atomic packing, and the direction is almost always the crystallographic direction of densest atomic packing (Schmid and Boas, 1935, p. 86, and Barrett, 1952, p. 338). The slip plane of zirconium, $\{10\bar{1}0\}$, is not the densest packed plane, but the slip direction, $\langle 11\bar{2}0 \rangle$, is in the direction of densest packing.

There are several methods of determining the slip direction by the use of x-rays (Maddin and Chen, 1954, pp. 68-72, and Hall, 1954, p. 35). However, the method used in this work was a modification of one described by Cahn employing microscopic examination of a deformed crystal (Cahn, 1951, pp. 20-21). The slip direction was found by making use of the fact that a crystal that has undergone slip shows no steps on a surface containing the slip direction. Thus on five of the crystals having a slip direction lying approximately in a surface, it was possible to establish the slip direction. The slip markings on the surfaces containing the slip direction were quite faint and difficult to see, whereas the slip traces on the adjacent faces were prominent and easily seen. In all five cases the direction was determined as $\langle 11\bar{2}0 \rangle$, which is consistent with the statement that the direction of closest packing is the slip direction. The direction of slip was determined by the use of stereographic projections of the crystals. It was possible to determine how nearly parallel the $\langle 11\bar{2}0 \rangle$ direction was to the surface showing faint markings by the use of the stereographic projections. In all the crystals in which the slip direction was reported, the $\langle 11\bar{2}0 \rangle$ direction was within fifteen degrees of being parallel to the surface, and in several cases it was within two degrees. The five crystals in which $\langle 11\bar{2}0 \rangle$ was determined to be the slip direction are B-21,

B-22, B-32, B-51, and B-52.

c) Determination of Critical Resolved Shear Stress for Slip

The critical resolved shear stress for slip is defined as that shear stress, resolved in the plane of slip and in the direction of slip, required to initiate slip. Experiments have been performed on many metals to find this quantity, and it has been found to be a constant for each metal. It does depend, however, on the condition of the crystals and on their purity. In metals containing more than one slip system the critical resolved shear stress may vary from slip system to slip system, but it is a constant within each system. More information concerning the general factors of this topic may be obtained from Barrett (1952) and from Schmid and Boas (1935).

Very often the critical resolved shear stress is computed from data obtained from a stress-strain curve of a single crystal deformed in tension. This curve shows a marked change in slope at the initiation of slip, and by suitable extrapolation a value for the axial stress at which slip first started may be obtained. This information, in conjunction with knowledge of the crystal orientation, is enough to allow computation of the critical resolved shear stress.

The crystals of zirconium used in this work were not thought to be long enough to employ the above method

satisfactorily. Instead, the method outlined below was used.

As the crystals of zirconium were too short to make reliable tensile tests, it was decided to compress single crystals for measurement of critical resolved shear stress. The principle of the measurement of the critical resolved shear stress was to obtain the axial force required to initiate visible slip. This axial force was resolved to give the shear stress in the plane of slip and in the direction of slip. This shear stress was taken to be the critical resolved shear stress. In some systems this is not a good method because slip occurs before the first slip traces become visible; however, in systems where the slip traces are well defined and rapidly increase in density with increasing deformation, this system is likely to be applicable (Orowan, personal communication, 1954). The slip traces in zirconium do increase in density rapidly with increasing deformation and the traces are quite prominent, as may be seen in the series of photographs of Figure 18. The relative constancy of the resolved shear stress as determined by this method with four crystals tends to strengthen the assumption of the validity of the method.

The actual testing of the single crystals was done in the compression apparatus previously discussed in the Description of Apparatus and Materials, and pictured in Figures 5, 6, 7, and 8. A microscope was used to examine

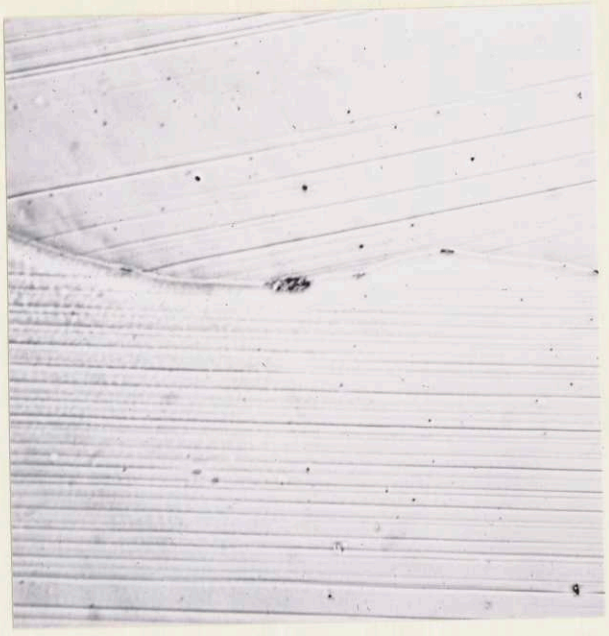

(A)

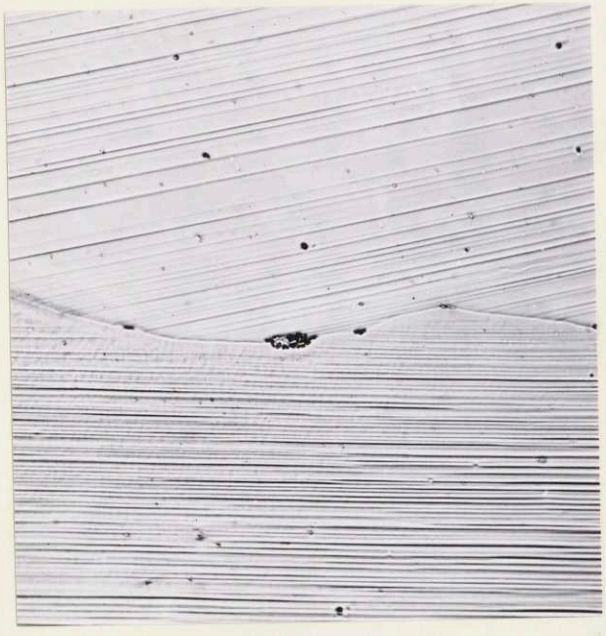

(B)

(C)

Figure 18: Slip in zirconium crystal
at various gross strains.
(A) 0.55 percent (B) 1.4 percent
(C) 2.2 percent. 160x.

the surfaces of the samples for the first visible traces of slip while the load was being applied. The loading was often interrupted to allow a static examination of all the sides of the compression sample. Loading was continued until evidence of slip was first observed, and the load was then determined and recorded. The samples were removed from the apparatus and examined in a metallograph for analysis of the slip plane. The samples were then replaced in the compression apparatus and loading continued until a new active plane was observed, and then the sample was again removed and examined metallographically.

The cross-sectional areas of the specimens were obtained in several ways. One method used was direct measurement of the transverse dimensions with a micrometer, coupled with knowledge of the dihedral angles between faces. On the compression samples an optical comparator was used to obtain images of the ends of the specimens, and the average area for each sample was taken as the mean area of the two ends. The area was found on some samples by measuring the mass of the sample and its length, and using this data with the tabulated density of zirconium (Russell, 1954, p. 1047) to compute an average area. These methods all checked with one another to approximately one half percent of the mean cross-sectional area.

Some of the compression samples were oriented so that twins were produced soon after visible slip. These samples

were used for measurements of twin indices. The samples used for measurement of the critical resolved shear stress for slip of $\{10\bar{1}0\}$ showed traces of only one set of parallel planes in the initial stages of slip. Use of these samples avoided the complications of cross slip and prior twinning in computation of the critical resolved shear stress. The critical resolved shear stress observed was about 0.65 Kg/mm^2 in compression on the slip system of the type $(10\bar{1}0)$ $[\bar{1}2\bar{1}0]$.

Quantitative data on the critical resolved shear stress was also obtained in tension. A single sample containing two usable grains (B-23a and B-23b), each about three-eighths of an inch long, was pulled in tension. The grips and loading was as pictured in Figure 4. The critical resolved shear stress observed was about 0.4 Kg/mm^2 in tension on the slip system of the type $(10\bar{1}0)$ $[\bar{1}2\bar{1}0]$.

It is to be noted that there is a difference between the values of critical resolved shear stress for slip as reported in tension and compression samples. It is probable that the values obtained in compression represent the more accurate data, for there is greater possibility of extraneous stresses in the tensile tests. Such extraneous stress concentrations may arise at grain boundaries, or in bending moments from imperfectly aligned tensile grips. This second possibility is given some

credulity by the fact that the initial slip traces in both crystals in the tensile bar were found to be located off to one side of the sample.

The slip traces in the compression samples appeared to be homogeneously spaced along the length of the sample, indicating that no major stress concentrations were present in the crystal. It is believed, therefore, that the values for the critical resolved shear stress for slip obtained from the results of the compression tests are more reliable than those from tension tests.

2. Analysis of the Crystallography of Twinning

a) Description of the Twinning Process

In the close-packed hexagonal metals twinning is an important mode of deformation. In zirconium this importance is magnified because there are more twin systems operative than in most of the other close-packed hexagonal metals. Therefore, a brief summary of the crystallography of the twinning process is given in the following pages.

The mineralogist Dana (1922, p. 160) has defined a twinned lattice as one in which, "One or more parts, regularly arranged, are in reverse position with respect to the other part or parts." This means that the twinned and untwinned portions of a lattice are mirror reflections of one another in a specific plane. This plane is called the twin plane, or the composition plane. Figure 19 (A) shows diagrammatically the results of a simple twinning process in a two dimensional lattice.

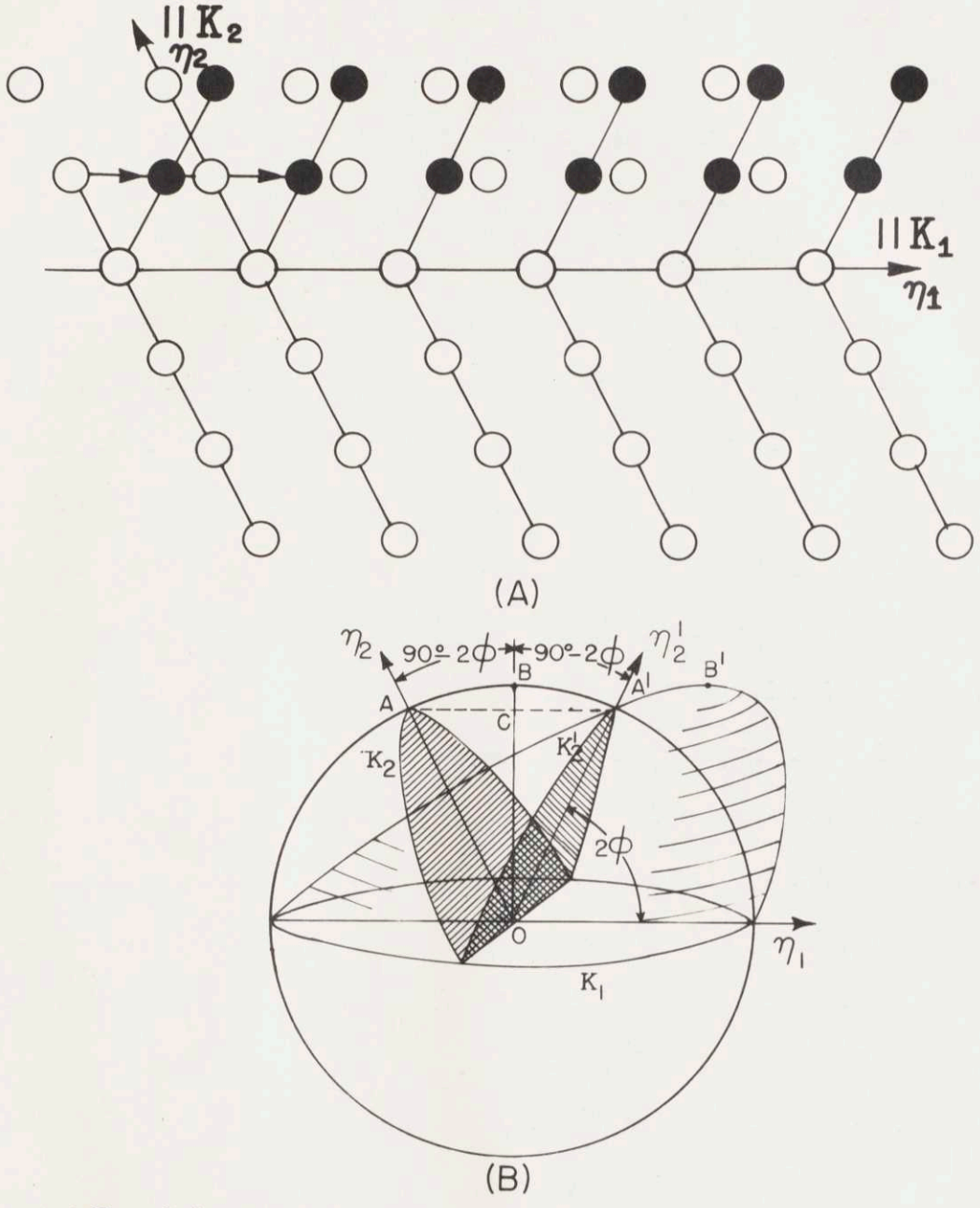

Fig. 19. (A) Illustration of formation of twin in a two dimensional lattice by uniform shear.

(B) Relationship of twinning geometry (Hall, 1954).

The indices of twinning are given in Figure 19(B). This figure represents a hypothetical single crystal originally in the shape of a sphere. The upper half of this sphere was then twinned with respect to the lower half. For the purposes of definition this twin may be considered to be the product of a homogeneous, or uniform, shear. The twinned portion of the solid figure is a part of an ellipsoid and has the same volume as it had prior to twinning. In Figure 19 the composition, or twin, plane is given as K_1 and the direction of shear in this plane is η_1. K_1 is an undistorted plane in the shear process. A second undistorted plane is given by the intersection of the surface of the ellipsoid after twinning, and the surface of the sphere before twinning. This plane is denoted as K_2^1 and is the twinned position of the plane K_2. The direction η_2 in the plane K_2 may be defined as the intersection of K_2 and the "plane of shear," which is formed by η_1 and the normal to K_1. The shear, $\underline{S}$, may be given by the expression

$$S = 2 \cot 2\phi$$

where $\underline{2\phi}$ is the acute angle between K_1 and K_2.

A combination of several of the parameters described above is necessary for the complete definition of the crystallography of a twin. Very often only K_1 is found, but it is necessary to obtain enough of the other indices to make the geometry of Figure 19 determinate, to completely define the twin.

Homogeneous shear on an atomic scale for the twin formation was assumed for purposes of definition; however, in the general case twinning of a lattice does not occur by this process. The end result of twinning yields a gross or macroscopic geometry that may be described by a homogeneous shear, but the detailed movement of the atoms in the twinned portion of the lattice in most cases does not appear to be a homogeneous shear. The macroscopic shear seems to be related to the shear of a certain group of space lattice points within the crystal. These specific space lattice points within themselves undergo what appears to be a uniform shear, and they are defined by the following conditions (modified from Hall, 1954, p. 48).

1) If A and B are two space lattice points, which after the uniform twinning shear are mutual reflections in the composition plane, then before twinning the line joining them must be parallel to η_2.
2) The line AB is bisected by the composition plane, K_1.

The atoms that have not participated in the uniform shear movement must, presumably, move in such a fashion to end up with the lattice restored in the twinned portion of the crystal after twinning. This may involve movements of atoms in directions other than η_1, and even in planes

other than K_1.

Twins are often classified by the relationships of K_1, η_1, K_2, and η_2. Twins of the first type are those having rational indices for K_1 and η_2, and irrational indices for K_2 and η_1. This type is the most general in minerals. Type II twins have rational indices for K_2 and η_1; and K_1 and η_2 are irrational. Reciprocal twins are a pair of twins in a lattice, one of which is a type I twin having values of K_1 and η_2 which are the same as K_2 and η_1 of the second twin, which is type II. Twins occurring in crystals of high lattice symmetry often have all four indices rational and are termed "rational twins" or "compound twins." Most of the twins occurring in metals are rational twins.

b) Determination of Twinning Indices

The composition plane, K_1, is the easiest twin parameter to obtain. This plane is most often found by the two surface method or single surface method described in the section on Determination of Slip Plane. Other methods are discussed by Hall (1954) and Cahn (1954).

The other parameters of twinning found in this work were obtained from optical goniometric measurements of the deformation produced in the surfaces of samples that had been twinned. A description of these various methods of analysis follows. Some of these give the shear and η_1 and some give additional indices; however, specification

of $\underline{K_1}$, $\underline{\eta_1}$, and $\underline{S}$ completely defines the twin system.

A method of using metallographic measurements of the distortion of the crystal surface to determine the twin indices is also discussed. This method served as an independent check on the goniometric data.

Figure 20 and Figure 21 show the parameters used in two methods of vector analysis devised to obtain the twin indices and shear associated with twinning. Figure 20 (A) is a perspective drawing of a twinned crystal, and Figure 20(B) and (C) are normal projections of the crystal faces I and II. The faces I and II were sheared in twinning to form the surfaces Ia and IIa. The trace of Ia on I makes an angle α^I with the reference edge and this trace is given by the vector $\overline{A}$. The similar situation on face II gives the vector $\overline{B}$. The sheared surface Ia makes an angle γ^I with face I, and IIa makes an angle γ^{II} with II.

The projections of the crystal faces I and II given in Figure 20(B) and (C) give the vectors $\overline{A}$ and $\overline{B}$ correctly; however, they give projections of the true angle between the original edge and the sheared edge. These projected angles are given as θ^I and θ^{II}. A photograph of the face of a crystal containing a twin which sheared the reference edge is given for illustration in Figure 22.

Figure 21 is a diagram of the geometry of the twinning shear. The plane of the diagram is the plane defined by the shear direction, η_1, and the normal to the composition plane. The portion abcd of the crystal has twinned to

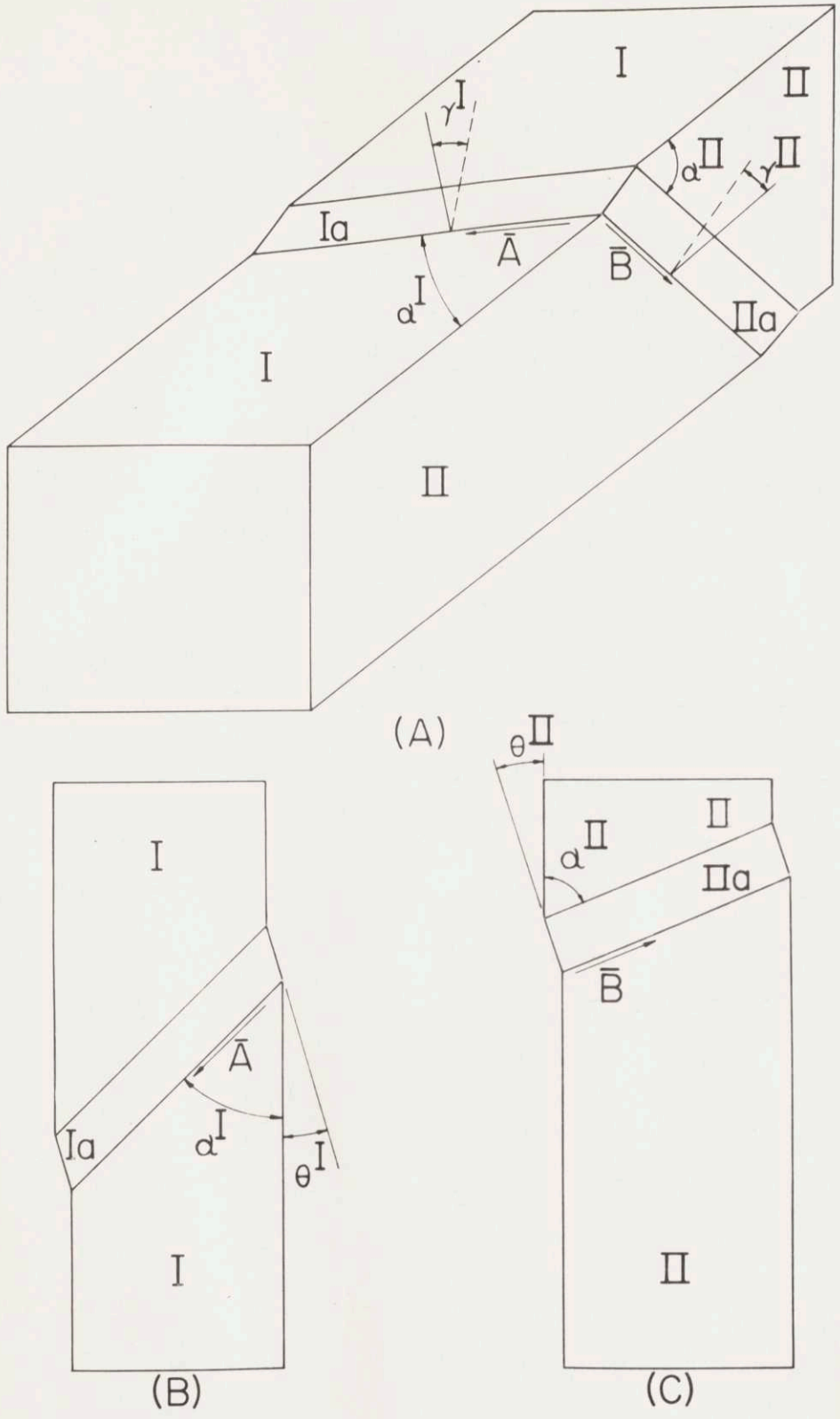

Fig. 20. Perspective of a twinned crystal (A) and normal projections of two of the twinned faces, (B) and (C).

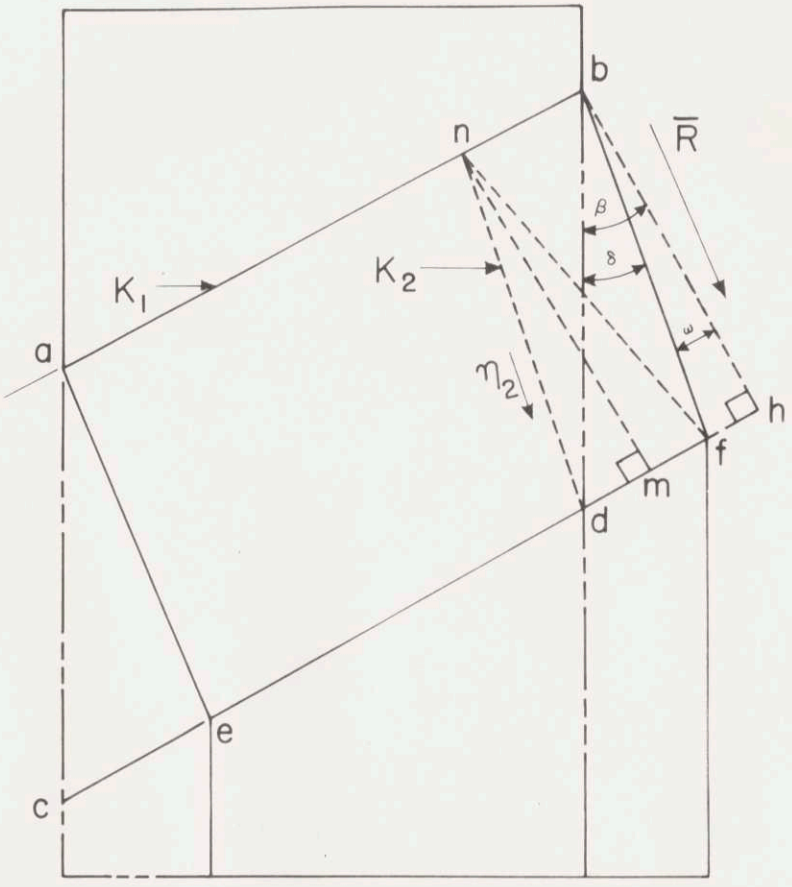

Fig. 21. Diagram of geometry associated with twinning shear.

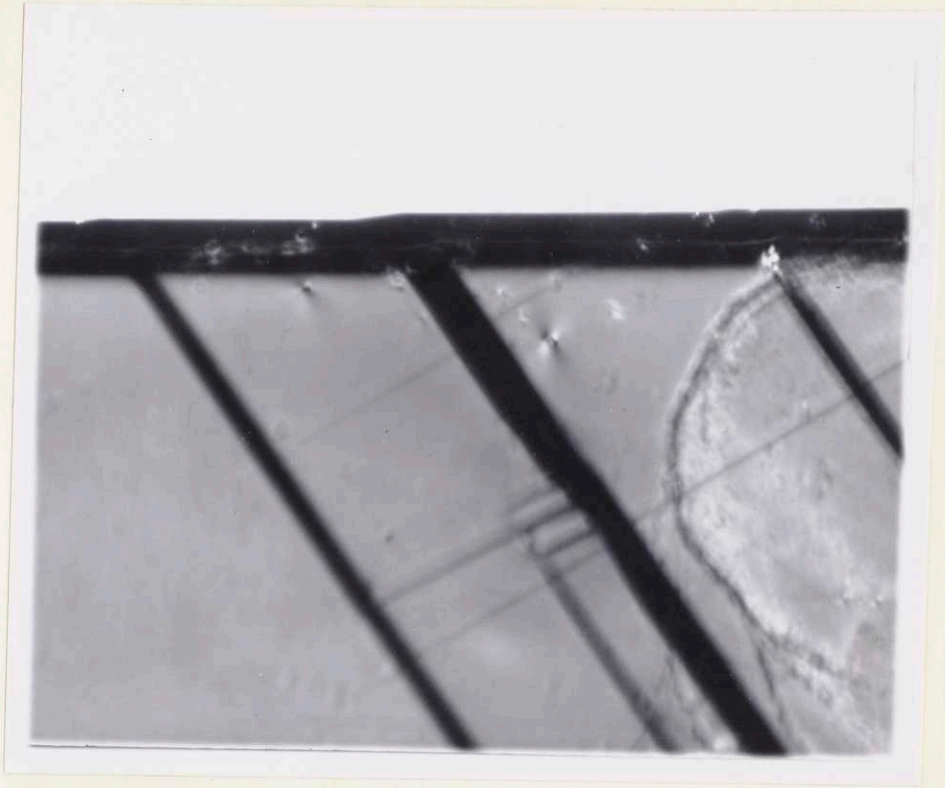

Figure 22: Photograph of twins intersecting the reference edge of a crystal to produce a sheared edge. Twins are {1122} twins. 200x, polarized light

become abfe. The line bd is the projection of the reference edge on this plane before twinning, and the line bf is the projection of this same edge after twinning. Thus, the shear associated with twinning may be obtained by dividing the shear distance df, by mn, the normal distance from df to the twin interface, ab.

The first method of vector analysis to find the shear of twinning utilizes measurements of γ^{I}, γ^{II}, α^{I}, and α^{II} as given in Figure 20. From these measurements and a knowledge of the crystal orientation, one may obtain the twin indices, K_1, η_1, K_2, η_2, the shear, and the shear

angle, $90^\circ - 2\phi$. This method of analysis is outlined below along with a second method which uses measurements of θ^{I}, θ^{II}, α^{I}, and α^{II}, as shown in Figure 20.

1) Vector Analysis of Twin Indices from Measurements of γ^{I}, γ^{II}, α^{I}, α^{II}

(A) Define vectorially the surfaces I, Ia, II, and IIa, by their normals, $\bar{I}$, $\bar{Ia}$, $\bar{II}$, and $\bar{IIa}$, respectively, which are vectors of arbitrary length (see Figure 20). It is to be noted that surfaces I and II are not necessarily perpendicular to one another.

(B) $$\bar{I} \times \bar{II} = \bar{R_o}' ; \quad \bar{I_a} \times \bar{II_a} = \bar{R}' \qquad (1)$$

where $\bar{R_o}'$ = a vector in direction of original reference edge

$\bar{R}'$ = a vector in direction of sheared reference edge

(C) Obtain the normal to the twin plane from the relation

$$\bar{A} \times \bar{B} = \bar{N} \qquad (2)$$

where $\bar{A}$ = a vector of arbitrary length in direction of twin trace in I (defined by measurement of α^{I})

$\bar{B}$ = a vector of arbitrary length in direction of twin trace in II (defined by measurement of α^{II})

$\bar{N}$ = a vector in direction normal to twin plane

(D) Consider the twin formed, with its parallel faces shearing the reference edge $\underline{\bar{R}_o}'$ to a new position, $\underline{\bar{R}}'$. Let vector $\underline{\bar{R}_o}$ (which is parallel to $\underline{\bar{R}_o}'$) be what was the position of the original reference edge between the parallel faces of the twin. Let $\underline{\bar{R}}$ be the vector that is generated when $\underline{\bar{R}_o}$ is sheared to its new position. ($\underline{\bar{R}}$ is in the direction of $\underline{\bar{R}}'$). Thus the magnitudes of $\underline{\bar{R}_o}$ and $\underline{\bar{R}}$ are not arbitrary.

Thus $\underline{\bar{\eta}_1}$, the direction of shear, is given by the relation

$$\underline{\bar{\eta}_1} = \underline{\bar{R}} - \underline{\bar{R}_o} \tag{3}$$

and the shear may be defined by

$$S = \frac{|\bar{\eta}_1|}{|\bar{R}_o| \cos \epsilon} \tag{4}$$

where S = shear

ϵ = angle between $\bar{R}_o$ and $\bar{N}$; hence

$$\cos = \frac{\bar{R}_o' \cdot \bar{N}}{|\bar{R}_o'||\bar{N}|}$$

(E) The relation between $\underline{\bar{R}}$ and $\underline{\bar{R}_o}$ may be obtained by setting the projection of $\underline{\bar{R}}$ on $\underline{\bar{N}}$ equal to the projection of $\underline{\bar{R}_o}$ on $\underline{\bar{N}}$. This is true because $\underline{\bar{R}}$ was formed from $\underline{\bar{R}_o}$ by a simple shear process. Thus one may obtain the following relationship for $\underline{\bar{R}}$

$$\bar{R} = \left[\frac{(\bar{R}_o \cdot \bar{N})}{(\bar{R}' \cdot \bar{N})}\right] \bar{R}' = k\left[\frac{(\bar{R}_o' \cdot \bar{N})}{(\bar{R}' \cdot \bar{N})}\right] \bar{R}' \qquad (5)$$

where $\bar{R}_o = k\,\bar{R}_o'$

(F) One may then combine equations (3) (4) and (5) and obtain S and η_1.

$$S = \frac{|\bar{\eta}_1|}{|\bar{R}_o| \cos\epsilon} = \frac{|(\bar{R} - \bar{R}_o)|}{|\bar{R}_o| \cos\epsilon} = \frac{\left|\left[\frac{(\bar{R}_o' \cdot \bar{N})}{(\bar{R}' \cdot \bar{N})} \bar{R}' - \bar{R}_o'\right]\right|}{|\bar{R}_o'| \cos\epsilon}$$

$$= \left|\left[\frac{\bar{R}'}{(\bar{R}' \cdot \bar{N})} - \frac{\bar{R}_o'}{(\bar{R}_o' \cdot \bar{N})}\right]\right| \cdot |\bar{N}| \qquad (6)$$

(G) Inasmuch as each vector occurring in the numerator of (6) occurs also in the denominator, the final expression for shear is independent of the magnitudes chosen for the direction vectors $\bar{R}_o'$, $\bar{R}'$, and $\bar{N}$. Since $\bar{R}_o'$, $\bar{R}'$, and $\bar{N}$ are obtained from γ^I, γ^{II}, α^I, and α^{II} the shear is obtained from these primary measurements.

(H) From the parameters S, η_1, and the knowledge of K_1 (obtained from step (C)), one may deduce all the other twin indices.

2) Vector Analysis of Twin Indices from Measurements of θ^I, θ^{II}, α^I, α^{II}

In principle this method is the same as the method outlined above. The difference between the two methods is that in this case one uses θ^I and θ^{II} to determine the

vector $\underline{\bar{R}'}$, the sheared edge, whereas in the above method one uses $\underline{\gamma^{I}}$ and $\underline{\gamma^{II}}$. A photograph of a twinned sample from which measurements of $\underline{\theta^{I}}$ and $\underline{\theta^{II}}$ were taken is shown in Figure 22.

Since $\underline{\theta^{I}}$ is the angle formed by the reference edge, $\underline{\bar{R}_{o}'}$, and the projection of $\underline{\bar{R}'}$ on surface $\underline{I}$, and a similar situation holds for $\underline{\theta^{II}}$ on surface $\underline{II}$, one has enough information to formulate the vector $\underline{\bar{R}'}$. This may be seen by noting that one may obtain two spacial coordinates for $\underline{\bar{R}'}$ from each value of $\underline{\theta}$, and by making the common coordinates equal, the three space coordinates defining $\underline{\bar{R}'}$ are obtained. Having found $\underline{\bar{R}'}$ one may follow the method given above in the analysis from measurements of $\underline{\gamma^{I}}$ and $\underline{\gamma^{II}}$.

3) Stereographic Analysis of Twin Indices from Measurement of γ^{I}, γ^{II}, α^{I}, α^{II}

The following method of stereographic analysis of the twin indices from measurements of $\underline{\gamma^{I}}$, $\underline{\gamma^{II}}$, $\underline{\alpha^{I}}$, and $\underline{\alpha^{II}}$ was obtained from work done by Greninger (1949, pp. 596-597) and by Hall (1954, pp. 54-55). The stereographic solution for the twin indices is given in Figure 23. In this figure, the plane of projection is the twin or composition plane. The other indices are noted on the diagram.

The steps in the stereographic solution are as follows:

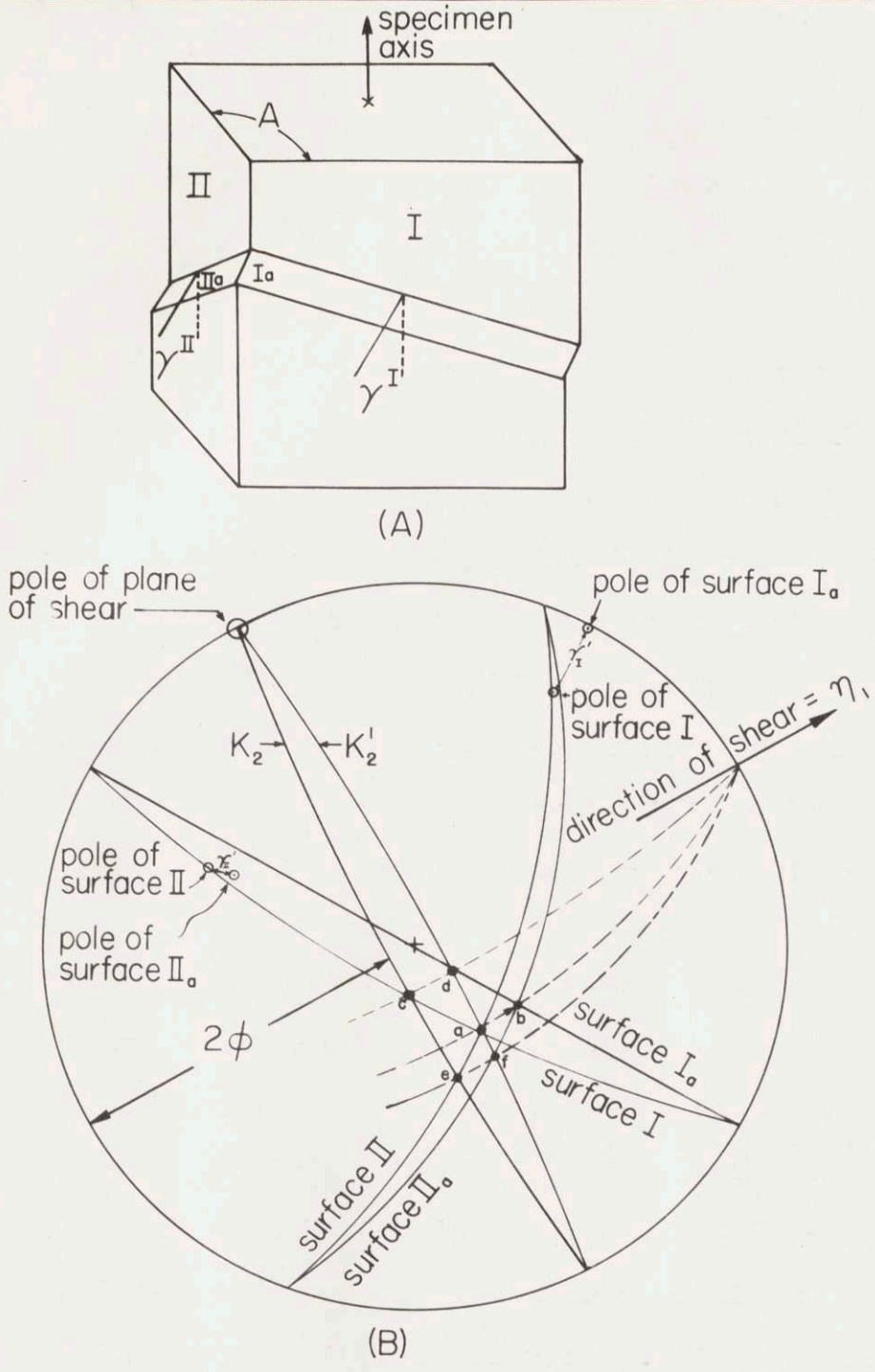

Fig. 23. (A) Twinned crystal with sheared surfaces.

(B) Stereographic analysis of twinning indices. K_1 is plane of projection.

1) Plot the poles of I, Ia, II, and IIa on a stereogram of the crystal, using surface I as the projection plane.

2) Rotate the projection to make the twin plane, K_1, the plane of projection.

3) On the projection given in step (2) plot the surfaces I, Ia, II, and IIa as great circles. This stage is shown in Figure 23.
I and II intersect at $\bar{R}_o'$, given as a in Figure 23.
Ia and IIa intersect at $\bar{R}'$, given as b in Figure 23.
The line connecting a and b in the stereogram lies on a great circle and goes in the direction of shear, η_1.

4) To evaluate 2ϕ, the Wulff net is rotated on the projection until the shear direction, η_1, coincides with the equator of the net, and then K_2 and K_2' are found by using the requirement that K_2 and K_2' must be at equal angles from the normal to K_1. Since K_2 and K_2' intersect I, Ia, II, and IIa, the requirement may be made that points c and d must be equal angles from the projection normal, and the same must be true for e and f. 2ϕ is then given as the angle between K_2 and K_1.

(5) The remaining twin parameters may easily be obtained from those derived in the above analysis.

4) Goniometric Measurement of γ^{I} and γ^{II}

The angle between the surface of the untwinned portion of the crystal and the twinned portion of the crystal was measured on several faces of each crystal. These angles are the angles γ^{I} and γ^{II} given in Figure 20, and a description of the method of measuring them is given below.

The samples were mounted in a goniometer and positioned so that an incident beam of light was reflected from the sample surface into the low-power microscope. The plane defined by the incident light beam and the reflected beam was made perpendicular to the twin trace on the surface of the sample. The angles γ^{I} and γ^{II} were then found, on their respective surfaces, by rotating the sample about an axis through the twin trace until one had obtained a reflection of the light beam into the microscope by both the surface of the untwinned portion, and the twinned portion, of the crystal. The difference in angle of the occurrence of these two reflections gave directly the angle between the two surfaces.

One must take care to keep the light beam well collimated and fairly fine. The source should also be far enough away so that the change in position of the sample as it is rotated does not affect the geometry by an appreciable amount.

The method described above is an excellent method for the measurement of γ^{I} and γ^{II} so long as the width of the sheared surface, Ia, formed by the twin is large with

respect to the wavelength of the light used. As the width of the sheared surface approaches the wavelength of light, one obtains a diffracted beam that diffracts through a larger and larger angle.

The angle defined by the first minima of the diffracted beam from a twin trace is given by the expression:

$$\theta = 2 \sin^{-1} \frac{\lambda}{w}$$ (Born, 1951, pp. 76-79)

where θ = angle of divergence of diffracted beam

λ = wavelength of incident light

w = width of reflecting surface

This effect can become quite important as the twins become thinner. It was this effect that limited the precision of the determination of the shear in the $\{11\bar{2}1\}$ twin system.

If one assumes a wavelength of about 5000 angstroms, and widths of the various twin systems corresponding to widths calculated from the photomicrographs of Figure 24, one obtains the approximate values of $\underline{\theta}$ shown in Table V.

Table V: Widths, and calculated values of the angle of divergence, of twin planes of zirconium.

Twin Plane	Width of Trace (microns)	Angle of Divergence θ (degrees)
$\{10\bar{1}2\}$	41	$1\frac{1}{2}$
$\{11\bar{2}2\}$	12	5
$\{11\bar{2}1\}$	2	29

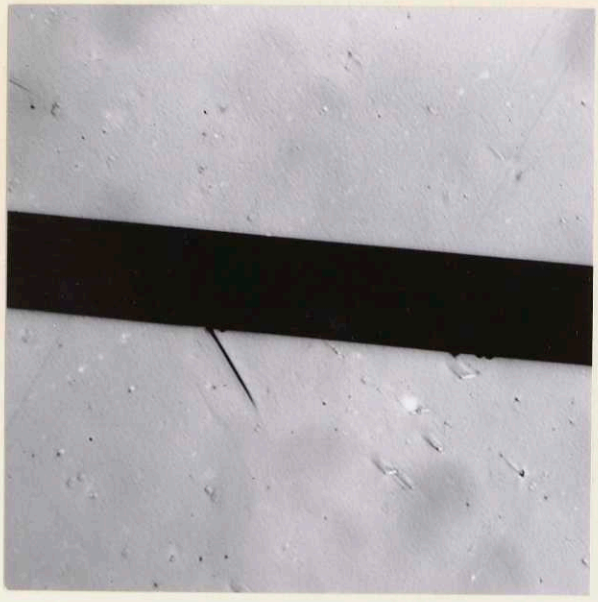

(A)

(B)

(C)

Figure 24: Typical appearance of twins in zirconium. (A) $\{10\bar{1}2\}$, (B) $\{11\bar{2}2\}$, (C) $\{11\bar{2}1\}$. 300x, polarized light.

The goniometric measurements were satisfactory for the $\{10\bar{1}2\}$ twins and the $\{11\bar{2}2\}$ twins because the divergent beam was narrow enough to select a reasonable intensity maximum. However, the angle of divergence was too great on the $\{11\bar{2}1\}$ twins to obtain good measurements, and because of this, the shear measurement and the determination of the other indices of twinning are relatively uncertain for this twin type. Uncertainty in measurement of very narrow twins has also been experienced by Cahn (1951) and Paxton (1953).

c) Discussion of the Application of the Methods of Determination of Twin Indices

Three methods of analysis of twin indices were presented in Determination of Twin Indices. Two of these methods were vector methods of similar derivation, but using different data, and one method was a stereographic method. One vector analysis method and the stereographic analysis method utilize the same measurements of $\underline{\gamma}^{I}$, $\underline{\gamma}^{II}$, $\underline{\alpha}^{I}$, and $\underline{\alpha}^{II}$ (shown in Figure 20). The stereographic method is perhaps less precise than the vector method, but it is often quicker and easier. The stereographic method also has the advantage of allowing one to see the crystallographic neighborhood of the derived indices, and thus obtain a better overall view of the twinning process. This virtue also allows the smoothing of slightly faulty data. If the initial measurements are sufficiently accurate, however, the vector method will give the values of shear

and $\underline{2\phi}$ to greater accuracy than does the stereographic method.

The second vector method, which uses measurements of $\underline{\theta}^{I}$, $\underline{\theta}^{II}$, $\underline{\alpha}^{I}$, and $\underline{\alpha}^{II}$ (shown in Figure 20, is useful in several respects. It is of use first as an independent check on the other two methods because it is based on measurements of different angles. This method may also be of use on crystals which do not lend themselves to the measurement of $\underline{\gamma}^{I}$ and $\underline{\gamma}^{II}$. This may occur if many different twins are formed, making the surface a poor reflector. Another advantage of this method is that all the angles used in it may be found using only a metallograph with a revolving stage. The measurement of $\underline{\gamma}^{I}$ and $\underline{\gamma}^{II}$ in the other methods requires careful determination on an optical goniometer or similar instrument.

VI. Results and Discussion of Results

Fourteen zirconium crystals, selected on the basis of size and quality, were deformed: nine in tension, and five in compression. From the deformation of these crystals, information on the deformation processes of zirconium was obtained. A stereogram showing the orientation of the axes of the crystals used is given in Figure 12. Table VI, Table VII, and Table VIII summarize the experimental data on the slip systems and twin systems observed in these crystals of zirconium.

A. Slip and Twinning Systems

The planes found to be active as twinning planes in each of the crystals tested are shown in Table VI. A summary of the data concerning slip in the crystals tested is given in Table VII. The critical resolved shear stresses for slip, given in Table VII, were obtained on crystals which had slip occurring as the only visible deformation mode in the initial stages of plastic deformation.

A summary of experimentally determined twin indices is given in Table VIII. Indices of $\{10\bar{1}2\}$ and $\{11\bar{2}2\}$ twins have been determined by vector analysis from both goniometric data and metallographic data, and also by stereographic analysis using goniometric data. The twin indices found by these methods checked with one another, and the shears found experimentally agree to less than three degrees with the calculated shears obtained using

Table VI: Active twinning planes in zirconium crystals deformed in tension and compression at room temperature.

Crystal	Direction of Stress	Magnitude of Max. Gross Strain - %	Observed Twin Planes K_1 Values			
A-21a	tension	10	$\{10\bar{1}2\}$	$\{11\bar{2}1\}$	--	$\{11\bar{2}3\}$
A-21b	tension	10	$\{10\bar{1}2\}$	$\{11\bar{2}1\}$	$\{11\bar{2}2\}$	$\{11\bar{2}3\}$
A-21c	tension	10	$\{10\bar{1}2\}$	$\{11\bar{2}1\}$	$\{11\bar{2}2\}$	--
A-21d	tension	10	$\{10\bar{1}2\}$	$\{11\bar{2}1\}$	--	$\{11\bar{2}3\}$
A-21e	tension	10	$\{10\bar{1}2\}$	$\{11\bar{2}1\}$	--	--
B-21	compression	< 0.1	--	$\{11\bar{2}1\}$	--	--
B-22	compression	< 0.1	--	$\{11\bar{2}1\}$	--	--
B-23a	tension	< 0.1	--	--	--	--
B-23b	tension	< 0.1	--	--	--	--
B-24a	tension	< 0.1	$\{10\bar{1}2\}$	$\{11\bar{2}1\}$	--	--
B-24b	tension	< 0.1	--	--	--	--
B-32	compression	< 0.1	--	$\{11\bar{2}1\}$	$\{11\bar{2}2\}$	--
B-51	compression	< 0.05	--	--	--	--
B-52	compression	< 0.05	--	--	--	--

Table VII: Summary of slip deformation on crystals of zirconium tested in tension and compression at room temperature.

Crystal	Length inches	Raw Material	Direction of Stress	Slip Plane	Slip Direction	Shear Stress Resolved in Slip Direction and Plane (Kg/mm^2)
A-21a	3/8 (c)	crystal bar	tension	$\{10\bar{1}0\}$	(a)	(b)
A-21b	3/16 (c)	crystal bar	tension	$\{10\bar{1}0\}$	(a)	(b)
A-21c	1/4	crystal bar	tension	$\{10\bar{1}0\}$	(a)	(b)
A-21d	3/16	crystal bar	tension	$\{10\bar{1}0\}$	(a)	(b)
A-21e	1/8 (c)	crystal bar	tension	$\{10\bar{1}0\}$	(a)	(b)
B-21	3/8	arc-melted	compression	$\{10\bar{1}0\}$	$\langle 11\bar{2}0\rangle$	0.69 ± 0.10
B-22	3/8	arc-melted	compression	$\{10\bar{1}0\}$	$\langle 11\bar{2}0\rangle$	0.70 ± 0.10
B-23a	1/2	arc-melted	tension	$\{10\bar{1}0\}$	(a)	0.4
B-23b	5/16	arc-melted	tension	$\{10\bar{1}0\}$	(a)	0.4
B-24a	1/2	arc-melted	tension	$\{10\bar{1}0\}$	(a)	(b)
B-24b	3/16	arc-melted	tension	$\{10\bar{1}0\}$	(a)	(b)
B-32	1/2	arc-melted	compression	$\{10\bar{1}0\}$	$\langle 11\bar{2}0\rangle$	(b)
B-51	3/4	arc-melted	compression	$\{10\bar{1}0\}$	$\langle 11\bar{2}0\rangle$	0.61 ± 0.05
B-52	5/8	arc-melted	compression	$\{10\bar{1}0\}$	$\langle 11\bar{2}0\rangle$	0.62 ± 0.05

(a) probably $\langle 11\bar{2}0\rangle$, but not determined
(b) not determined
(c) grain did not extend completely around sample

Table VIII: Summary of twin indices of twinned zirconium crystals deformed in tension and compression at room temperature.

Crystal	Twin Indices*				Calculated Shear Parameters for Given K_1, η_1, K_2		Experimental Shear Parameters	
	K_1	η_1	K_2	η_2	S	$90^\circ-2\phi$	S	$90^\circ-2\phi$
B-24a	$(10\bar{1}2)$	$[\bar{1}011]$	$(10\bar{1}\bar{2})$	$[10\bar{1}1]$	0.167	4.8°	(a) 0.190 (b) 0.210 (c) 0.154	5.5° 6° 4.4°
B-32	$(11\bar{2}2)$	$[\bar{1}\bar{1}23]$	$(11\bar{2}\bar{4})$	$[\bar{2}\bar{2}43]$	0.225	6.4°	(a) 0.246 (b) 0.252 (c) 0.245 (d) 0.228 (e) 0.280	7° 7.2° 7° 6.5° 8°
B-21	$(11\bar{2}1)$	(f)	(f)	(f)	(f)	(f)	(g) 0.35	(g) 10°
B-22	$(11\bar{2}1)$	(f)	(f)	(f)	(f)	(f)	(g) 0.35	(g) 10°

* See Figure 19 for nomenclature of indices
(a) Shear found on stereogram, from γ^{I} and γ^{II} (see Figure 20)
(b) Shear found by vector analysis from θ^{I} and θ^{II} (see Figure 20)
(c) Shear found by vector analysis, from γ^{I} and γ^{II} (see Figure 20)
(d) Shear analysis for second set of planes in sample B-32, from stereogram, using γ^{I} and γ^{II}
(e) Shear analysis for second set of planes in sample B-32, vector analysis using γ^{I} and γ^{II}
(f) Not definitive because shear measurement inaccurate since γ^{I} and γ^{II} only approximate
(g) Approximate values because small size of twin caused uncertainty in γ^{I} and γ^{II}

the known crystal geometry and the experimentally obtained values of $\underline{K_1}$, $\underline{\eta_1}$, and $\underline{K_2}$.

Although measurements were attempted to determine the twin indices of $\{11\bar{2}1\}$ twinning, the data obtained was not reliable. These twins were so thin that the beam of light incident on their surface traces was diffracted over a large angle (see Table V). Because of this diffraction effect, only an approximate value for the twinning shear of $\{11\bar{2}1\}$ twins was obtained.

Figure 25 is a diagram of the crystallography of $\{10\bar{1}2\}$ twinning. In this diagram, part (A) shows the twin plane, $(10\bar{1}2)$, and the plane of shear, $(1\bar{2}10)$, in a hexagonal cell. Part (B) of Figure 25 is a projection of the plane of shear, $(1\bar{2}10)$, showing the positions of the space lattice points in that plane. The uniform shear component of motion is shown by the arrows which go from the initial space lattice positions (open circles), to the final twinned positions (filled circles). The twin indices are drawn in the diagram so that the twin is completely described.

The projection of the uniform shear component of $\{11\bar{2}2\}$ twinning is given in Figure 26. The projection plane of this diagram is $(\bar{1}100)$ and again the initial and final positions of the space lattice points in the uniform shear are denoted by open and closed circles respectively. In this case it is to be noted that not all the space lattice positions on the projection can undergo homogeneous shear. The space lattice positions that do take part

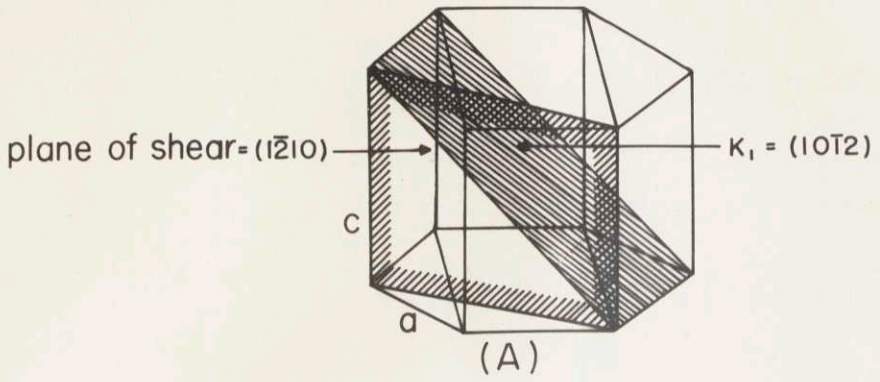

(A)

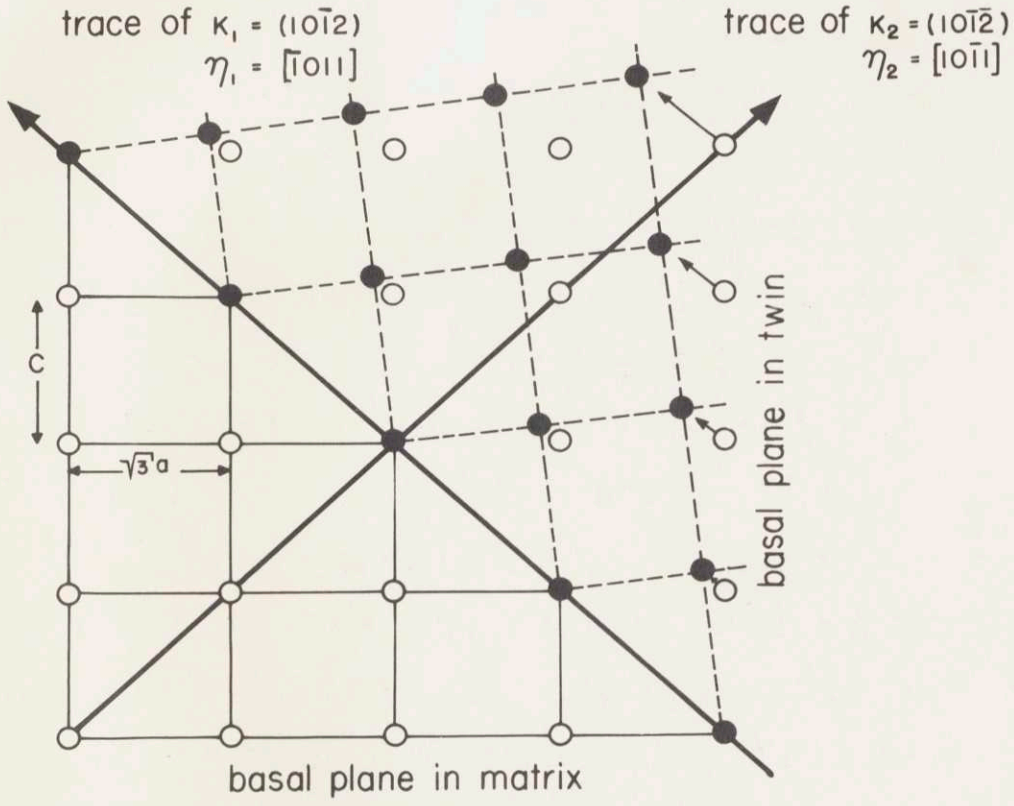

○ = untwinned space lattice point positions

● = twinned space lattice point positions from homogeneous shear

(B)

Fig. 25. (A) (10$\bar{1}$2) twin and (1$\bar{2}$10) shear plane in the hexagonal cell.

(B) Diagram of crystallography of homogeneous shear component of (10$\bar{1}$2) twinning in zirconium. Projection plane is (1$\bar{2}$10).

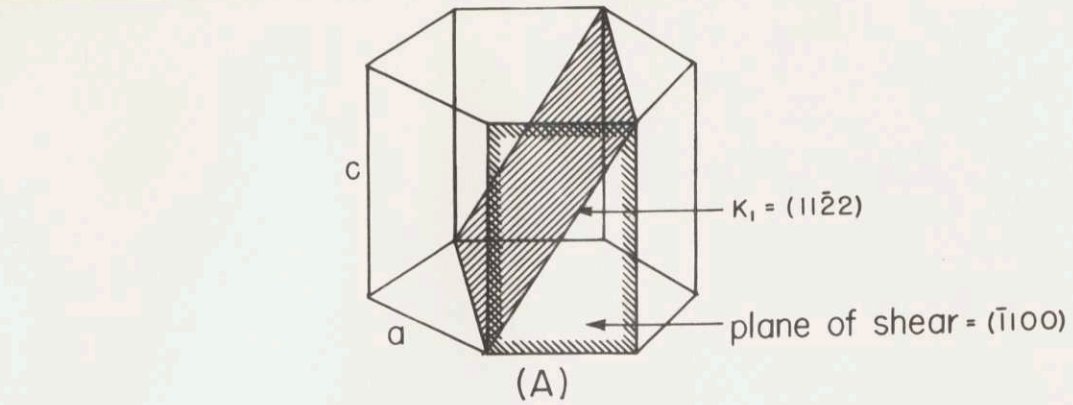

(A)

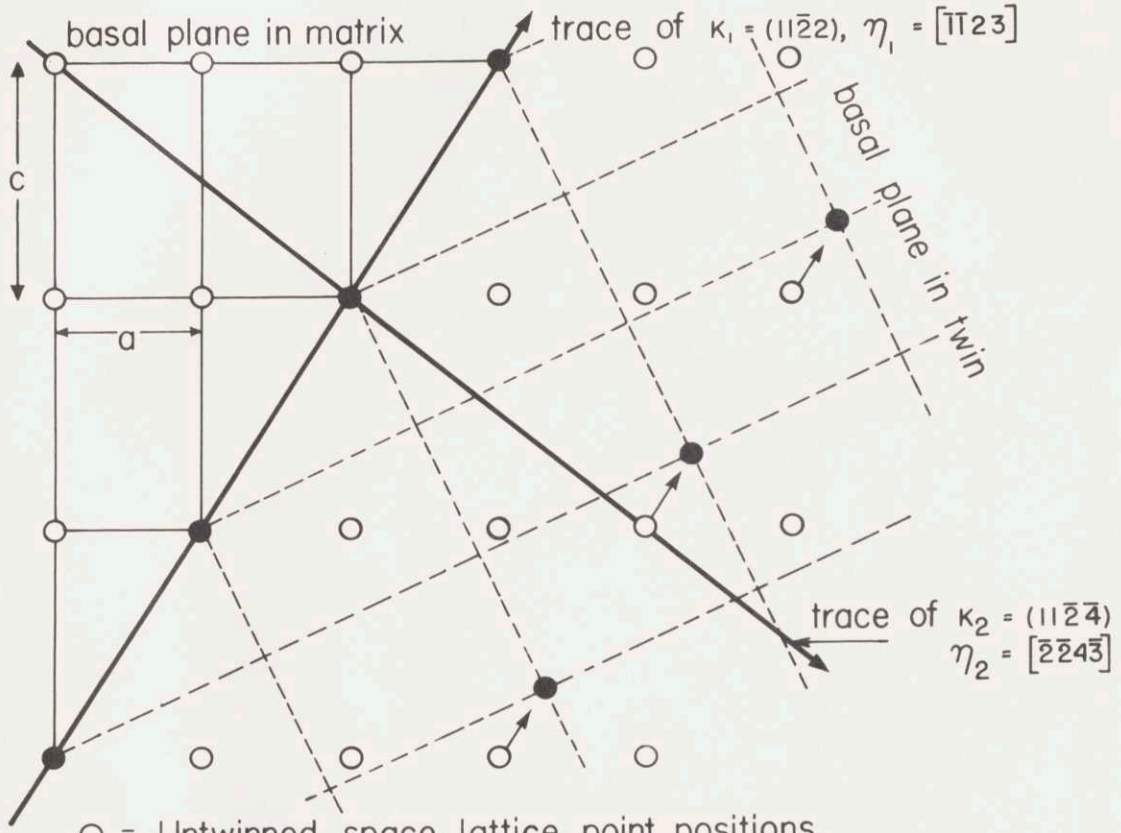

(B)

Fig. 26. (A) $(11\bar{2}2)$ twin and $(\bar{1}100)$ shear plane in the hexagonal cell.

(B) Diagram of crystallography of homogeneous shear component of $(11\bar{2}2)$ twinning in zirconium. Projection plane is $(\bar{1}100)$.

in the homogeneous shear deliniate a cell that is a multiple of the unit cell in the hexagonal close-packed structure. Thus, presumably, only a fraction of the space lattice points take part in the uniform shear displacement.

One of the important features of twinning with respect to the mechanical working of metals is that it reorients a portion of a crystal so that further deformation by slip might occur (Barrett, 1952, p. 378). Thus, a knowledge of the orientation of the twinned lattice with respect to the applied forces would be useful in deformation studies. One way to give this information is to give the angle between the c axis of the untwinned part of the crystal and the c axis of the twinned part of the crystal. The twinning relationship between these two axes requires that the two be mirror images of one another in the twin plane. Therefore, the angle between the two c axes is twice the angle between the c axis and the twin plane. Since the angles between the c axis and the poles of the twin planes are known, the angles between the two c axes are readily calculated. This information is tabulated in Table IX for the twins of zirconium.

Table IX: Angles between c axis of untwinned portion of zirconium crystal and c axis of twin for various twins,

Twin Plane	Angle Between c Axis and Pole of Twin Plane (degrees)	Angle Between c Axis of Untwinned and Untwinned Parts of Crystal (degrees)
$\{10\bar{1}2\}$	42.61	85.22
$\{11\bar{2}1\}$	72.58	34.84
$\{11\bar{2}2\}$	57.88	64.24
$\{11\bar{2}3\}$	46.72	86.56

B. Relationship of Twinning Shear and Twin Thickness

Figure 24 shows photographs of $\{10\bar{1}2\}$, $\{11\bar{2}1\}$, and $\{11\bar{2}2\}$ twins. These photomicrographs are all shown at 300 diameters and were taken with polarized light. The thickness of the twinned portion of the crystal remained roughly constant for each family of twins from test to test, and from sample to sample. The absolute thickness, as calculated from the projected thicknesses of Figure 24, are given in Table X along with the value of shear for each twin family.

Table X: Twin thickness and twinning shear for $\{10\bar{1}2\}$, $\{11\bar{2}1\}$, and $\{11\bar{2}2\}$ twins in zirconium.

Twin	Twinning Shear (S)	Twin Thickness (microns)
$\{10\bar{1}2\}$	0.167	31
$\{11\bar{2}2\}$	0.225	10
$\{11\bar{2}1\}$	0.35 (a)	2

(a) approximate value

It may be seen from the data in Table X that as the magnitude of the twinning shear increases, the thickness of the twin decreases. Cahn (1951, pp. 30-32) has reported this observation and has offered several possible explanations for it.

One tentative explanation that may be put forth here is based on the premise that the layers of atoms in twins of higher shear have greater barrier energies to overcome in going to twin positions than do layers of atoms in twins of lower shear. It would be expected that atoms which move closer to their neighbors in a shear movement would have a higher barrier energy than atoms that do not pass so closely to their neighbors. This is consistent with the observation that the larger the shear, the closer the shearing atoms have to pass each other; i.e. the interatomic distances in the structure momentarily attained when the shear is half completed, are reduced with respect to the normal values, and that fractional reduction is the greater, the greater the shear (Cahn, 1951, p. 32).

One may postulate that the energy reservoir for twinning, i.e. the elastic energy within the crystal, is roughly the same for all the twin families. It would then be expected that layer after layer of atoms would shear, drawing energy from this reservoir, and the process would stop when the energy level of the reservoir dropped to the level of the barrier energy. Thus more layers would shear in

twins of low barrier energy than in twins of high barrier energy. Since twins of low barrier energy are presumably twins of low shear, one may expect these to be thicker than twins of high shear.

C. Kinking

Kinking was observed near the grain boundaries of some of the grains pulled in tension to a strain of 10.7 percent. Kinking was also seen in samples that had been deformed by bending; however, no kinking was observed on the tension or compression samples that were only slightly deformed.

D. Notes on Twin Formation

The twins in these experiments were all formed under stress; that is they are all mechanical twins. Subsequent annealing of twinned crystals did not seem to promote growth of twins; in fact, twins subjected to annealing seemed generally to be consumed. No annealing twins were observed in zirconium. Some twins were produced by abrasion on emery paper, but no analysis was made to determine the families of these twins.

The twins formed under stress always yielded a "cry" or "click" during their formation, and these twins always were formed after an interruption in the loading. This interruption came about when the loading was stopped for inspection of the specimen surfaces for deformation traces. Very often, twinning would occur immediately upon resumption of loading.

The broader twins, $\{10\bar{1}2\}$ and $\{11\bar{2}2\}$, often had small flaws in their sides. Photomicrographs of twins showing some of these flaws may be seen in Figure 24. These two twin families also seemed to have more of a tendency to end in the volume of a crystal than did the other twins.

VII. Conclusions

1. After removal of hydrogen, zirconium single crystals can be produced by one of two techniques. One is to heat the samples *in vacuo* for eight to ten days at 840° C; the other is to cycle the samples *in vacuo* several times between four hours at 1200° C and five to ten days at 840° C.

2. Slip has been observed at room temperature only on the system $(10\bar{1}0)\ [\bar{1}2\bar{1}0]$, in crystals of relatively high purity. The critical resolved shear stress for $\{\bar{1}0\bar{1}0\}$ slip is about 0.65 Kg/mm^2 for single crystals tested in compression, the lowest value observed being 0.61 Kg/mm^2. No basal slip has been observed in any of the crystals tested, the crystals tested representing a fairly complete coverage of orientations.

3. Deformation twins having composition planes of $\{10\bar{1}2\}$, $\{11\bar{2}1\}$, $\{11\bar{2}2\}$, and $\{11\bar{2}3\}$ are observed in zirconium crystals tested at room temperature. Complete specification of twin parameters is given for $\{10\bar{1}2\}$ and $\{11\bar{2}2\}$ twins and an approximate shear magnitude has been obtained for $\{11\bar{2}1\}$ twins.

4. The shear values of $\{10\bar{1}2\}$, $\{11\bar{2}2\}$, and $\{11\bar{2}1\}$ twins are found to increase in the above order, whereas the absolute thickness of the twinned layer decreases in the above order.

5. Two methods of finding the twin indices by vector analysis have been developed, and their application discussed. The two methods utilize independent observations and may yield greater accuracy than is obtained by stereographic analysis.

6. A design for apparatus to perform quantitative compression testing on single crystals has been presented.

VIII. Suggestions for Further Work

The following are some suggestions for further work in the study of the deformation of zirconium:

1. An investigation into the slip processes of zirconium containing interstitial impurities, to determine the possible occurrence of such additional slip planes as $\{10\bar{1}1\}$ and (0001). This study might also include the determination of the variations of critical resolved shear stress with temperature.

2. An investigation into the inverse relation between the macroscopic twinning shear of the various twins and the thickness of the twinned layer. A study of the variation of twin occurrence and twin thickness with temperature might be included.

3. Determination of the remaining twin indices of the $\{11\bar{2}1\}$ and $\{11\bar{2}3\}$ twin planes.

4. Development of a method for producing larger single crystals of alpha zirconium.

IX. Biographical Note

The author was born March 13, 1930 in St. Louis, Missouri. He attended the public schools of St. Louis and University City, Missouri. After graduating from University City Senior High School in 1948, he attended Massachusetts Institute of Technology. He was married in the summer of 1950, and received a Bachelor of Science Degree in Metallurgy from Massachusetts Institute of Technology in 1952. In the fall of 1952 he began graduate studies at Massachusetts Institute of Technology.

His professional experience includes three years at the M.I.T. Metallurgical Project as a Division of Industrial Cooperation employee, and as a full, and half-time research assistant in the Department of Metallurgy, Massachusetts Institute of Technology. A fourth year of experience at this project was gained after it was changed to Nuclear Metals, Inc. He is a member of Tau Beta Pi and Sigma Xi.

X. Bibliography

Anderson, E. A., Jillson, D. C., and Dunbar, S. R., "Deformation Mechanisms in Alpha Titanium," Journal of Metals, Vol. 5, No. 9, Sept. 1953, 1191-1197.

Barrett, Charles S., "The Crystallographic Mechanisms of Translation, Twinning and Banding," Cold Working of Metals, Cleveland, American Society for Metals, 1949, 65-98.

Barrett, Charles S., Structure of Metals, Second edition, New York, McGraw-Hill Book Company, 1952.

Born, Max, Atomic Physics, Fifth edition, London, Blackie and Son Limited, 1951.

Brick, R. M., Lee, H. T., and Greenewald, H. Preparation of Single Crystals of Beryllium and Zirconium; Study of Mechanical Properties, University of Pennsylvania, Quarterly Report, July 1, to Sept. 30, 1950.

Burgers, W. G., "On the Process of Transformation of the Cubic-Body-Centered Modification Into the Hexagonal-Close-Packed Modification of Zirconium," Physica, Vol. I, 1934, 561-586.

Cahn, R. W., Plastic Deformation of Uranium, United States Atomic Energy Commission Technical Information Service, AERE-M/R-740, 1951.

Cahn, R. W., "Plastic Deformation of Alpha Uranium; Twinning and Slip," Acta Metallurgica, Vol. I, No. 1, January 1953, 49-70.

Cahn, R. W., "Twinned Crystals," Advances In Physics, Vol. 3, No. 12, October 1954, 363-445.

Churchman, A. T., "The slip modes of titanium and the effect of purity on their occurrence during tensile deformation of single crystals," Proceedings of The Royal Society, Series A, Mathematical and Physical Sciences, Vol. 226, No. 1165, Nov. 9, 1954, 216-226.

Clark, R., and Craig, G. B., "Twinning," Progress in Metal Physics, ed. Bruce Chalmers, Volume 3, London, Pergamon Press Ltd., 1952, 115-139.

Dana, E. S., A Textbook of Mineralogy, Third edition, New York, John Wiley & Sons, Inc., 1922.

Greninger, A. B., and Troiano, A. R., "The Mechanism of Martensite Formation," Transactions of American Institute of Mining and Metallurgical Engineers, Volume 185, 1949, 590-598.

Hall, E. O., Twinning and Diffusionless Transformations in Metals, London, Butterworths Scientific Publications, 1954.

Liu, T. S., and Steinberg, M. A., "Twinning in Single Crystals of Titanium," Journal of Metals, Volume 4, Number 10, October 1952, 1043.

Luetzow, H. J., A Study of the Critical Strain of Zirconium, Argon National Laboratory, ANL 5164, 1953.

Maddin, R., and Chen, N. K., "Geometrical Aspects of the Plastic Deformation of Metal Single Crystals," Progress in Metal Physics, ed. Bruce Chalmers and R. King, Volume 5, London, Pergamon Press Ltd., 1954, 53-95.

McHargue, C. J., and Hammond, J. P., "Deformation Mechanisms in Titanium at Elevated Temperatures," Acta Metallurgica, Volume 1, Number 6, November 1953, 700-705.

Miller, G. L., Zirconium, New York, Academic Press Inc., 1954.

Paxton, H. W., "Experimental Verification of the Twin System in Alpha Iron," Acta Metallurgica, Volume 1, Number 2, March 1953, 141-143.

Rosi, F. D., Dube, C. A., and Alexander, B. H., "Mechanism of Plastic Flow in Titanium-Determination of Slip and Twinning Elements," Journal of Metals, Volume 55, Number 2, February 1953, 257-265.

Russell, R. B., "Coefficients of Thermal Expansion for Zirconium," Journal of Metals, Volume 6, Number 9, September 1954, 1045-1052.

Schmid, E., and Boas, W., Plasticity of Crystals, London, F. A. Hughes & Co. Ltd., 1950, Translated from Kristallplastizitaet, 1935.

Schwartz, C. M., and Mallett, M. W., Observations on the Behavior of Hydrogen in Zirconium, Cleveland, American Society for Metals, 1953, Preprint number 14.

Tuer, George, Fundamental Mechanical and Physical Characteristics of Beryllium as Related to Single Crystals, Sc.D. Thesis, Department of Metallurgy, Massachusetts Institute of Technology, 1954.